Peltier Module in Effect to Extract Safe Water from Atmospheric Moisture Powered by Solar Photovoltaic Renewable Energy System with Contribution from Piezo-Materials

By

Mohammed Thushar Imran
18121018
Azraf Nafi Barshan
18121014
Sharif Mohd Shams
18121036
Rahat Tajwar
18121011

A thesis submitted to the Department of Electrical and Electronic Engineering in partial fulfillment of the requirements for the degree of
B.Sc. in Electrical and Electronic Engineering

Department of Electrical and Electronic Engineering
Brac University
September 2021

Declaration

It is hereby declared that

1. The thesis submitted is our own original work while completing degree at Brac University.
2. The thesis does not contain material previously published or written by a third party, except where this is appropriately cited through full and accurate referencing.
3. The thesis does not contain material which has been accepted, or submitted, for any other degree or diploma at a university or other institution.
4. We have acknowledged all main sources of help.

Student's Full Name & Signature:

Mohammed Thushar Imran	**Azraf Nafi Barshan**
18121018	18121014
Sharif Mohd Shams	**Rahat Tajwar**
18121036	18121011

Approval

The thesis/project titled "Peltier Module in Effect to Extract Safe Water from Atmospheric Moisture Powered by Solar Photovoltaic Renewable Energy System with Contribution from Piezo-Materials" submitted by

1. Mohammed Thushar Imran (18121018)
2. Azraf Nafi Barshan (18121014)
3. Sharif Mohd Shams (18121036)
4. Rahat Tajwar (18121011)

of Summer, 2021 has been accepted as satisfactory in partial fulfillment of the requirement for the degree of B.Sc. in Electrical and Electronic Engineering on [September 28, 2021].

Examining Committee:

Supervisor:
(Member)

____
Dr. A. K. M. Abdul Malek Azad
Professor
Department of Electrical and Electronic Engineering BRAC University, Dhaka.

Program Coordinator:
(Member)

____
Abu S.M. Mohsin, PhD
Assistant Professor
Department of Electrical and Electronic Engineering,
BRAC University, Dhaka

Departmental Head:
(Chair)

____
Md. Mosaddequr Rahman, PhD
Professor and Chairperson
Department of Electrical and Electronic Engineering,
BRAC University, Dhaka

Ethics Statement

All resources and data used for our project have been treated as confidential. All the study and work have been voluntarily done by us. We have carefully observed and examined our data. No payment has been made to any person who will directly or indirectly be involved in this project work. We have avoided discrimination against our members and have focused on minimizing human and animal harms as much as possible and maximizing benefits.

Abstract

The progressing world have many problems and the demands of people are increasing day by day. The demand for electricity and pure water are mentionable among the very alarming issues. This paper describes the design of atmospheric water generator which is powered up by renewable sources of energy. To generate the power, we are producing electricity with application of solar panel, charge controller and lead acid battery to power up the atmospheric water generation system and along with that, piezoelectric elements mounted under tiles which lights up the digital voltmeter-ammeter display. The atmospheric water generation part consists of the Peltier effect of thermoelectric cooler associated with Heat sinks and a DC Fan. Both Hardware and Software designs are implemented for discussion. It includes comparative study of consumed power from the sources and the individual contribution of piezo elements and solar panel are verified. Moreover, the efficiency of methods concerning generating water with Peltier effect has been depicted through experiments.

Keywords: Piezoelectricity; Piezo materials; Hybrid Renewable Energy; Solar Panel; Peltier effect; Thermoelectric Cooler; Atmospheric Water Generation;

Dedication

This work is dedicated mainly to our parents for all their efforts and encouragement they have invested in us up until now. We also dedicate the work to our supervisor who has been more than a pillar in the development of the final work results.

Acknowledgement

We would like to express our gratitude to Dr. A K M Abdul Malek Azad, Professor, BRAC University, Department of Electrical and Electronic Engineering (EEE), for his assistance, guidance, and feedback for the completion of our thesis.

Table of Contents

Declaration ii

Approval iii

Ethics Statement iv

Abstract v

Dedication vi

Acknowledgement vii

Table of Contents viii

List of Tables xi

List of Figures xii

List of Acronyms xiv

Chapter 1 Introduction 1

1.1 Background 1

1.2 Literature Review 2

1.3 Motivation 4

1.4 Thesis Organization 5

Chapter 2 System Design 7

2.1 General Design Concept 7

2.2 Proposed Hardware design 7

2.3 Hardware Requirements 9

2.4 Software Requirements 14

Chapter 3 Renewable Energy Generation 16

3.1 Energy Generation from Piezo... 16

3.2 Characteristics Analysis Simulation of Piezo Material: 19

3.3 Energy Generation from Solar Panel 23

3.4 Complete Model Prototype 31

3.5 Result Analysis of Produced Electricity 32

Chapter 4 Atmospheric Water Generation 34

4.1 Working Principle of Peltier Device 34

4.2 Procedures in Efficiency Management 36

4.3 Data Collection Mechanism.. 36

4.4 Comparative Result Analysis of Consumed Water 44

Chapter 5 MATLAB Simulation and Results 48

5.1 Complete System Representation with Solar PV Panel... 48

5.2 Specifications of Parameters for Solar Panel.. 50

5.3 Result Analysis PV Panel Simulation.. 53

5.4 Relay based switching phenomena between battery and PV panel 56

5.5 Piezo Voltage and Current Generation Simulation.. 57

Chapter 6 Feasibility Analysis 60

6.1 Impact and Sustainability... 60

6.2 Applicable Standard and Codes 60

6.3 Risk Management and Safety Consideration... 61

Chapter 7 Conclusion and Future Work **62**

7.1 Summary 62

7.2 Future Work 62

Appendix **69**

A. Water accumulation rate plotting on MATLAB 69

B. Code for Temperature and Humidity Sensing with DHT11 70

C. MPPT algorithm for the specification Charge Controller 71

D. Code for relay switching 74

E. Similarity Index Report 76

List of Tables

Table 1: Complete List of Materials 13

Table 2: Day 1 (only with the prototype)...37

Table 3: Day 2 (Humidity and Temperature sensor incorporated and small container was used) 37

Table 4:Day 3 (Tried to make the whole system as closed as possible).................................38

Table 5: Day 4 Test with modifications..38

Table 6: Day 5 test (Complete Off grid Test) with modifications..39

Table 7: Comparison with Related Research of AWG system..45

Table 8: Averaged Hourly GHI (Wh/m2) of August (Summer) [28].....................................50

Table 9: Averaged Hourly GHI (Wh/m2) of January (Winter) [28] 50

List of Figures

Figure 1: Power Generation System for Piezo and Peltier 7

Figure 2: Atmospheric Water Generation Model 8

Figure 3: Piezo Element and Peltier Device (From left to right) 9

Figure 4: Solar PV Panel 10

Figure 5: Arduino Uno 11

Figure 6: DHT11 Sensor 11

Figure 7: Lead Acid Battery 12

Figure 8: Piezo Mounted under tiles 17

Figure 9: Rectifier circuit with capacitors connected on the load side. 18

Figure 10: Digital Voltmeter and Ammeter 19

Figure 11: Voltage and Current from Piezo mounted under tiles 19

Figure 12: Energy Harvester under varying stress (a function of frequency) 20

Figure 13: Energy Harvester under varying stress (a function of time) 21

Figure 14: Relationship of input mechanical power, the electric power (in mW) and the maximum induced voltage across the piezoelectric block (in V) as a function of frequency. 21

Figure 15: Relationship of input mechanical power, electric power and induced voltage with respect to a varying load resistance with a constant acceleration of 9.81ms^(-1) and oscillation at 70.5Hz. 22

Figure 16: Relationship of positive induced voltage on the electrodes, electric power and mechanical power as a function of acceleration (g) and the sinusoidal output voltage under a harmonic load as with respect to time 23

Figure 17: 65W-12V Solar Polycrystalline Solar 28

Figure 18: Solar Panel and Charge Controller Wiring Diagram 29

Figure 19: 12v-6A Charge controller, Battery and Load connection 29

Figure 20: Digital Voltmeter-Ammeter reading across load 30
Figure 21: Design Parts of the Hardware Prototype 31
Figure 22: Simulation result of temperature variation of hot and cold side of Peltier device [32] 35
Figure 23: Relationship of Relative Humidity and Temperature [35] 42
Figure 24: Amount of Water at 100% Relative Humidity [36] 42
Figure 25: Comparative analysis of water generation rate of Peltier module from experimental data 44
Figure 26: Integration of Solar Panel with Battery. 49
Figure 27: Average Daily GHI data of summer. (August) 51
Figure 28: Average Daily GHI Data of Winter. (January) 51
Figure 29: Average Daily Temperature Data of Summer (20th August, 2021) [38]...............52
Figure 30: Average Daily Temperature Data of Winter (20th January, 2021) [38] 52
Figure 31: Load current and load voltage simulation 53
Figure 32: Solar Panel Parameters Simulation 54
Figure 33: Battery parameters simulation..55
Figure 34: Relay switching circuit...56
Figure 35: energy harvesting circuit using piezoelectric element 57
Figure 36: The circuit diagram of LTC388-1 57
Figure 37: Output Voltage across the load 59
Figure 38: Output current through load 59

List of Acronyms

AC	Alternating Current
AWG	Atmospheric Water Generation
CFC	Chlorofluorocarbons
DC	Direct Current
HFC	Hydrofluorocarbon
PCB	Printed Circuit Board
PV	Photovoltaics
IWM	Institute of Water Modelling
WHO	World Health Organization

Chapter 1

Introduction

1.1 Background

It is a fact that, though 71 percent of the earth's surface is water, the scarcity of drinking water exists in many regions of the earth. According to WHO, a study from 2017 showed 29% of the global population lack pure drinking water and drinking water with presence of contaminants has accounted to cause 4,85,000 deaths on yearly basis due to diarrhea [1]. Moreover, it is estimated that by the year of 2025, half of people around the world will be in shortage of water. One of the most common sources of clean water is underground water but it is pumped at such a huge quantity that there is a big risk of land sink, building tilt and developing crack [2]. As per the data of the Institute of Water Modelling (IWM), the water table has risen by 50 meters when the past four decades are in consideration. The groundwater level which is supposed to be the closest is presently at a depth of over 60 meters all around different parts of Dhaka city. Here, the mean groundwater level varies as following- 11.3m in the year 1970, 26.6m in the year 1996, 28.15m in the year 1997, 30.45m in the year 1998, 31.85m in the year 1999, and 34.18m in the year 2000 [3]. In this very situation, extracting underground water can be a reason for greater damage than solving the clean water problem. In addition, many techniques require the usage of electricity for pumping underground water which can also be costly for many underdeveloped countries progressing at a fast pace. With the increasing population, the need for different resources is rapidly increasing. Electricity is a prime need in the modern era, still, a vast amount of electricity demand is met by natural materials like oil, coal and natural gas. The mentioned fossil fuels took about million years in forming but are finishing very rapidly since 85% of electricity is produced from non-renewable sources [4]. Recently, many successful attempts to introduce a range of renewable energies to create a more clean and efficient form of energy.

With this aim in mind, we are using systems consisting of piezoelectric materials and solar PV panel for the production of electricity. Due to global warming, the pure water supply has become another alarming concern. Using the Peltier effect, we are determined to generate water and accumulate a filtration system with it. Thus, the problem of shortage of pure drinking water and establishment of renewable energy generation systems will be holistically solved for creating a world with a more efficient way of living.

The overall objective of our project is to introduce these alternative sources for creating a world with more efficient ways of living. Our project aims to introduce a renewable source for power generation (piezo elements), adding another renewable source (Solar PV cell) to generate power and run an Atmospheric Water Generation (Peltier Module) system and meeting the demand for safe water.

1.2 Literature Review

The study of harvesting electrical energy from piezoelectric materials started off in the early 90s, in earlier studies, Sodano and Inman [5] encapsulated the significance of non-conventional sources of energy, videlicet, solar energy and direct piezoelectric effect, in response to startling depletion of fossil-fuel reserves and its adverse impact on the surrounding environment. They also briefed the maneuvers of piezo elements as sensors capable of transforming mechanical strain into electrical energy.

In the project report Solar Piezoelectric System [6], they have connected 5 piezo in series with full wave rectifier and capacitive filter. Thus, there will be a smooth DC supply and a capacitor connected to store input from piezo. It is controlled by relay and once the capacitor stores 15V, the relay sets to discharge the capacitor. The solar module and piezo are connected in parallel including a PCB for piezo system to minimize system loss here.

Yang [7], in an international journal, presented a detailed analysis on the piezoelectric energy harvesting and optimization techniques from the viewpoint of generating ample electric power under fluctuating excitation, and methodologies by coaxing the materials for achieving adequate output power. There has been a good amount of work on the optimization of piezoelectric sensors. Singh and Yadav [8] study manifested the synthesis and characterization of perovskite (BaTiO3) and its functionality as a sensor that encompasses the illustration of a 3-D critical structure of the material.

An AWG (Atmospheric Water Generator) system is obtainable using different techniques. The work of Anbarasu and Pavithra [9] depicts an AWG system composed of a dehumidifying section that exploits vapor compression refrigeration system. The bulkiness of the system and its characteristic of producing immense noise makes it very unsuitable to be installed in a car as it will put extra unnecessary weight on the vehicle and will create a vexing condition for the user.

According to a journal by Sajil et al. [10], it was seen that they produced at least 5ml water per hour using a single 4cm*4cm Peltier device. They have concluded the reason for low water production to be less surface area of the Peltier and the type of Peltier device that they used. Moreover, it was apprised that the Peltier device that was found in the market was not perfectly conditioned for the purpose of producing water. Therefore, it implies that by using larger surface area and a greater number of properly conditioned Peltier modules can increase the efficiency and effectiveness of producing water.

Niewenhuis et al. [11] brought about a wet desiccation system which was expected to compress moist air to an extent initiating the accumulation based on the surrounding temperature. The high pressure which will increase the dew point of the air is anticipated to cause a facile condensation process. Nevertheless, compressing the air to raise the dew point sufficiently will seemingly require pressure about 5 times the surrounding pressure. Ergo, it is crucial for the tank to be extraordinarily durable. Furthermore, the team has confirmed the system's inutility based on the synthesized results. Even though the prototype functions, it could only generate 0.72 liters of water per day.

Atta [12] developed the design structure of a water condensing system using thermoelectric coolers which got powered by Solar energy. The researcher came to realize the high installation cost for maintaining efficiency. Though he concluded how minimal requirements of maintenance, the cost savings can be experienced.

Kabeela et.al. [13], attempted to generate water from the atmosphere using a solar based dehumidification mechanism with the assistance of Peltier Device. It was patented that the usage of the Peltier Module made the system design more straightforward, increased portability and enhanced the environmental friendliness by avoiding noise pollution and by circumventing the need to use refrigerants such as CFCs and HFCs. In addition, the Peltier module operates directly from a DC source and has a wide range of input voltage and current.

1.3 Motivation

Taking all the information into consideration from the previous works, we have chosen the Peltier module for the condensation process as it has clearly stood out from all the other methods in terms of the simplicity of the design, mobility, robustness, and state of being eco-friendly. Besides, with consideration of emergence of new energy sources, we are implementing the use of piezoelectric properties. The conventional use of Solar PV panels is also showcased to give a concrete base to explore the new scopes with maximum efficiency.

1.4 Thesis Organization

The rest of the thesis writing is organized in the following order–

Chapter 2: *System Design*

In this chapter, the overall concept of the system design of Atmospheric Water Generation with Peltier Device along with Renewable Energy System was presented. Initially, the general concept was formed about how the connections will be made with solar and piezo which will power up the Peltier system and help in water generation. The hardware and software requirements for establishing the parts of electricity generation and water production was also discussed shortly in this chapter.

Chapter 3: *Renewable Energy Generation*

In Renewable Energy Generation chapter, we have showed how the model built with piezo elements and solar panel can work simultaneously in producing electricity. The concept of setting piezo in tiles and producing vibrations through steps for powering up voltage-current display is discussed in this chapter. Alongside with this, the solar panel is being set up as the main source for powering up the AWG.

Chapter 4: *Atmospheric Water Generation*

In this chapter, the working Peltier device along with Heat sink and 12V Fan is discussed elaborately. Different changes in design and how we achieved our maximum efficiency is mentioned in this chapter which we verified by changing different parameters and performing experiments. The discussion concluded with the best outcome and possibilities of improvement.

Chapter 5: *MATLAB Simulation and Results*

In MATLAB Simulation and Results chapter, we have discussed about our simulation of the entire system consisting both parts of our project. There were some restrictions in hardware implementation which we replenished with multiple testing from our simulated design. The data compiled here is finally compared with our hardware design. We improved the efficiency with our implemented design.

Chapter 6: *Feasibility Analysis*

In this chapter, we have discussed about the project's impact in economy also how our project contribution on economic sustainability. Next, we have discussed about how our project contribute in societal sustainability also the impact of the project in our society. We also discussed about the environmental sustainability and impact of our project. Moreover, we discussed about applicable standards and codes here we talked about what we have planned for our project and how we execute our plans step by step for our project. Finally, we have discussed about how we can ensure the user’s safety and take care of the risk management of our project.

Chapter 7: *Conclusion*

In this chapter, we go through the experience we achieved accomplishing this project and to what extent we have met our objectives. The socio-economic impact of the project in the society has also been analyzed. Besides that, the safety features and efficiency of our design has been reviewed . Finally, we stated in details our future work mentioning the improvements that can be done and how it can be made suitable for usage.

Chapter 2

System Design

2.1 General Design Concept

The design includes the main part of the project which determines the working principle of the whole structure. Starting from power generation to the final step is done precisely to give a visual representation both by hardware and software modeling.

The proposed system initially has a system with the combination of Solar Panel and Piezoelectric sensor in tiles. The Solar PV Panel supplies the major portion of power by generating required voltage and current which is connected to a charge controller and passes charge to a Lead Acid battery source. This turns on the Peltier device connected with a 12V DC fan and heat sinks. Finally, water gets condensed in a beaker with the mechanism of Peltier effect.

2.2 Proposed Hardware design

Initially, the power generation system is being established with along with the contribution of Piezo in lighting up voltage-current display and solar PV panel running the main load. Figure 1 explains the mechanism how the two different renewable energy sources are utilized for the project.

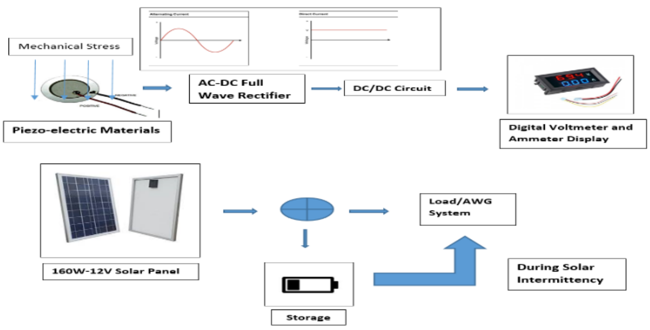

Figure 1: Power Generation System for Piezo and Peltier

The major part of hardware implementation is implementing the AWG with the help of Thermoelectric Cooler that exhibits Peltier effect. Two Heat Sinks on Hot and Cold Sides and Tapes are used to make structure for the prototype as shown in Figure 2. A beaker is used where the condensed water will get accumulated flowing through a small funnel wrapped with aluminum foil. The 12V Fan along with Peltier Device and Heat sinks is the core part of the prototype.

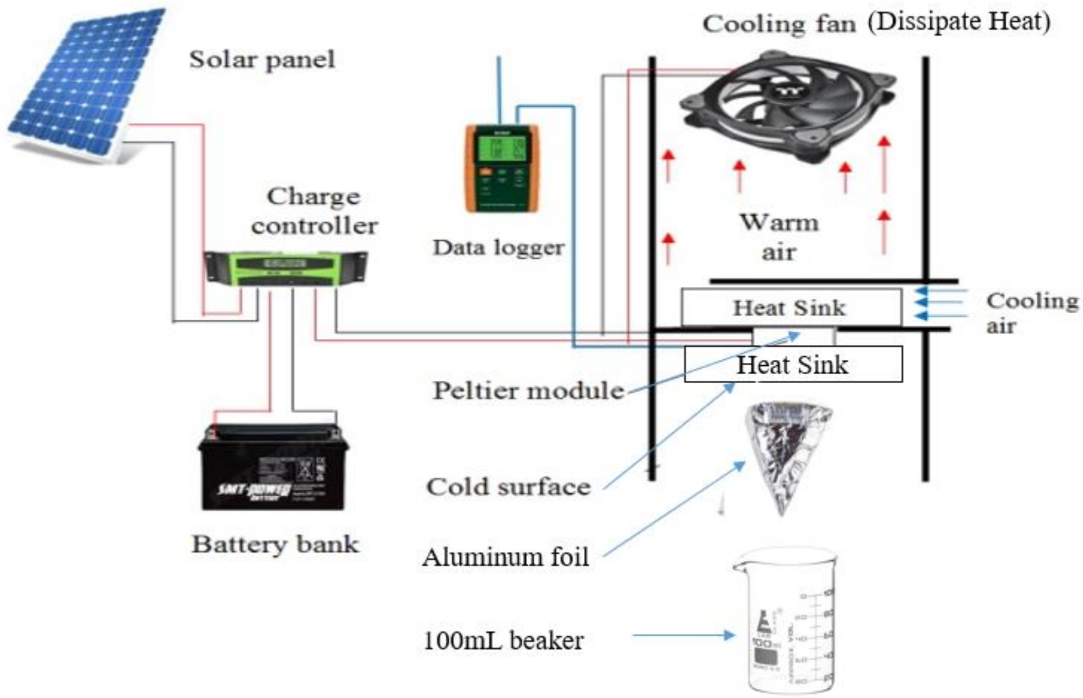

Figure 2: Atmospheric Water Generation Model

In addition to the basic setup, for calculation and testing purpose, Digital display and Arduino-run sensor DHT11 is used for temperature and humidity measurement making the system easier to understand and associate in data tracking to recording. With the complete demonstration, water gets accumulated in beaker and the subsequent readings related to the system are studied to clearly understand the efficiency of the accumulation.

2.3 Hardware Requirements

Figure 3: Piezo Element and Peltier Device (From left to right)

Peltier Device:

The Peltier module is a thermoelectric module which is made up of semiconductor materials having both n-type and p-type with the connection of electrical contact surfaces of metal. The two faces of the Peltier module are the two thermo coupled junctions [14]. The junction is in connection with the positive end of source is where the holes and electrons are flowing. As a result, creating a potential difference across the junction that causes the junction to absorb thermal energy (cooling effect) to balance the difference in the chemical potential of the two materials. Simultaneously, the junction connected to the negative terminal undergoes an opposite effect and becomes hot. The Peltier Module used in this project is of model TEC1-12706 as shown in the right side of Figure 3.

Piezo Elements:

Sensor made of Piezo elements uses the piezoelectric effect in order to detect variations in pressure application, acceleration phenomena, temperature effect, strain, or any similar force by turning them to the properties similar to that of an electrical charge [15]. The piezoelectric disc generates voltage when it is pressed or given constant taps. As shown in left of Figure 3, five piezo materials with a diameter of 35mm were used for the project.

Figure 4: Solar PV Panel

Solar Panel:

Solar Panels consist of Solar cells that do the conversion light energy into electrical energy through a phenomenon named photovoltaic effect. Thus, it is also known as photovoltaic cell. Fabricated silicon materials differentiate the solar panels in the classes like amorphous (non-crystalline), polycrystalline, or monocrystalline [16]. In this project, the used solar panel is poly crystalline silicon. The maximum power of the panel shown in Figure 4 is 65W and has system voltage maximum of DC 1000V. The open circuit voltage is 21V. The dimension of the panel is 660 x 550 x 30 mm.

Figure 5: Arduino Uno

Arduino Uno:

Arduino Uno is a microcontroller which has the ability to do different activities through generated codes and appropriate connections of sources and different type of sensors. Arduino programming language is set based on connections and thus required output is achieved [17]. The Arduino Uno used in the project (Figure 5) has the microcontroller board modelled ATmega328P. It has different digital and analog pins and also few inbuilt electronic components along with ports to give it the connection [18]. The Arduino works at 5V voltage and 16MHz. clock speed generated in it.

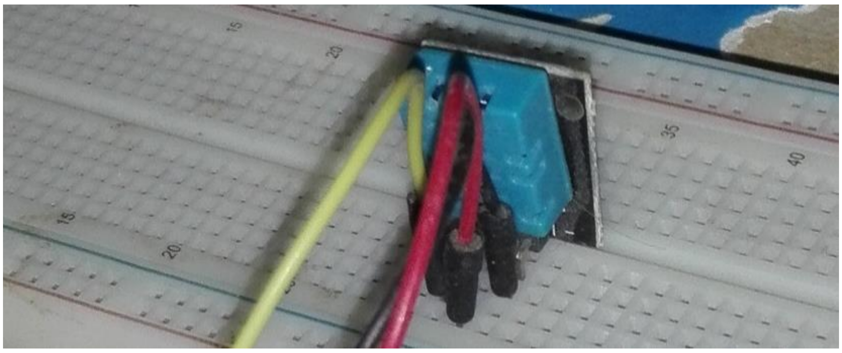

Figure 6: DHT11 Sensor

DHT11 sensor:

DHT 11 sensor of the Figure 6 is used for temperature and relative humidity sensing programming it with a microcontroller. It consists of humidity sensing elements capacitive in nature and for sensing temperature, a thermistor is also present. The IC made with the sensor and microcontroller does the work of changing these signals in digital signals [19]. It measures temperature with 2 degrees of accuracy in the range of 0 degree to 50 degree. Humidity is obtained with 5% accuracy in the range from 20% to 80%. In our prototype we had done coding for temperature in Celsius scale alongside with percentage of humidity and have run it by an Arduino.

Figure 7: Lead Acid Battery

Lead Acid Battery:

The Battery we used is a photovoltaic tubular deep cycle battery as per the Figure 7. This is mainly designed for running with solar panel supply along with the charge controller. Our used Lead Acid battery is of 12V and 30Ah. It has a slow discharge rate and completely discharges at 10 hours.

Complete List of Materials

Table 1: Complete List of Materials

Sl. No.	Products	Quantities
1.	Piezo element	5
2.	Peltier module	1
3.	Arduino Uno	1
4.	DHT11	1
5.	12V Battery Lead Acid Battery	1
6.	65W Solar Panel	1
7.	1N4007 Diode	5
8.	Capacitor	3
9.	Rectifier	5
10.	Mini Cooling Fan 40x40x10mm	1
11.	Aluminum Heat Sink	2
12.	Thermal Paste	1
13.	Breadboard Jumper Wire Set	1
14.	Gauge Wires Set	1
15.	Digital Voltmeter Ammeter	1

2.4 Software Requirements

MATLAB Simulink:

Simulink is a a design software from Matworks under MATLAB which is capable to work on different fields of electronic designing with block diagrams. It has different libraries based on the type of work one wishes to do and outputs in graphs, oscilloscope and other displays are easily demonstrated. When integreted with MATLAB code, it can do a range of variety functions for giving perfect idea with simulation befor hardware implementation **[20]**. Here the simulink library is used to demonstrate the full schematic configuration.

COMSOL Multi Physics:

For engineers and physicists, the COMSOL Multiphysics is a great software helping to study the characteristics analysis of different materials in the field of electronics. The software covers a huge domain of collection and parameter setting [21]. Here, it is used to study the properties of a Peltier Device through its explanation.

Proteus:

Proteus is used for block simulations and also in designing the PCB and 3D structure if needed for further analysis. The prototyping in Proteus ensures the maximum efficient design in software before approaching hardware design [22]. In the project, Proteus is used for testing purpose of circuit connections of Piezo and relay connection simulation which is considered future work of project.

LTspice:

LTspice is a software proffered by Linear Technology which allows us do simulations with various electronic components and special ICs made for different purposes. Moreover, they offer smart integration of RF ADCs, RF DACs, on-chip digital signal processing, and clock /PLL for multichip synchronization [23]. LTC3588-1 is an energy harvesting IC provided by Linear Technology which is available in LTspice library.

Chapter 3

Renewable Energy Generation

3.1 Energy Generation from Piezo

The advancement of wireless and micro electro-mechanical systems (MEMS) technology is followed by an ongoing surge of research on piezoelectric effect to provide an alternative to the conventional energy source (e.g., battery) to power up portable electronics devices. Naturally occurring materials, such as quartz, exhibit piezoelectric properties signifying the potential to transform external pressure into electrical energy that can be termed as the 'Direct Effect' as well as the 'Converse Effect' which does the opposite to 'Direct Effect', as a result of their crystalline structure [24]. One of the major fundamental characteristics of piezoelectric materials, a particular type of ferroelectric ceramic, functioning as PVDF (Polyvinylidene Fluoride) and Barium Titanate ($BaTiO3$) etcetera, is the random molecular orientation which appears to be a dipole ascribable to charge separation. Random orientation of the dipole opens into an insignificant net polarization of material whenever subjected to mechanical stress, hence induces a trivial amount of piezoelectric effect. To optimize the effect, the piezo-material is subjected to a process called poling that aligns the electric dipole excited through a strong electric field.

During poling, the electric dipole reorients relative to the electric field, and upon switching off the electric field, the material maintains a partially identical orientation as the electric field owing to a knock-on effect often termed as pinning effect generated by infinitesimal defects in the crystalline lattice . The off-centered position of the titanium ion induces an electrical polarity within the unit cell, thereupon triggering the electric dipole. If a mechanical stress exerts upon the crystal, it will reposition the titanium ion resulting in a variation in the polarization strength of the crystal which is the provenance of direct effect.

The piezoelectric effect comprises the direct effect that permits the external mechanical pressure to transform into electric energy and the opposite effect that enables the materials to function as an actuator. These effects can be modeled by two linearized consecutive equations [25]:

I. Direct piezoelectric effect: $\{D\} = [e]T\{S\} + [\boldsymbol{\alpha}S]\{E\}$ (1)

II. Converse piezoelectric effect: $\{T\} = [cE]\{s\} - [e]\{E\}$ (2)

Here, $\{D\}$ = the electric displacement vector,

$\{T\}$ = the stress vector,

$[e]$ = the matrix of dielectric permittivity,

$[cE]$ = the elastic coefficients matrix at fixed electric field force,

$\{S\}$ = the strain vector,

$[S]$ = the dielectric matrix at fixed mechanical stress, and

$\{E\}$ = refers the electric field vector [25] .

Figure 8: Piezo Mounted under tiles

We have attempted to harvest energy and power up a digital voltmeter and ammeter from the vibration or the pressure exerted on the piezoelectric element. The digital voltmeter and ammeter have been used to keep track of the voltage and the current across the AWG system. 5 circular piezoelectric elements of diameter 35mm were mounted under a tile as demonstrated on Figure 8. Energy could be generated when a person walks over the tile. From our experiment we found out that a single piezoelectric element can generate up to 40V, but can generate current within mA range. Since we get sufficient voltage but less current, we focused on increasing the current of the system. In order to increase the current, we just simply connected 5 piezoelectric elements in parallel.

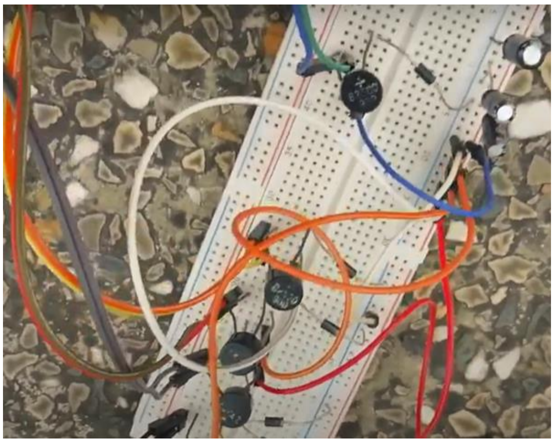

Figure 9: Rectifier circuit with capacitors connected on the load side.

When the piezoelectric element experiences enough on and off pressure, it generates fluctuating alternating voltage. In order to convert the alternating current to direct current we have connected a full wave rectifier across each piezoelectric element (shown on Figure 9). Moreover, to ensure steady current we have connected 3 capacitors of 47uF in parallel. Therefore, the total capacitance on the load side was 141uF. We tried to keep the capacitance high enough to reduce the ripples as we know that high RC value will increase the time taken for the capacitor to discharge.

Figure 10: Digital Voltmeter and Ammeter

Using this set up we tried to power up a digital voltmeter and ammeter of supply voltage of 3.5 – 30V as shown on Figure 10. Since the meter has a range of supply voltage that is suitable to withstand the voltage generated by the piezoelectric element, we did not have to use any buck boost converter and also using any converter would unnecessarily consume power.

Besides, the current and voltage reading practically without load are as follows,

Figure 11: Voltage and Current from Piezo mounted under tiles

We have applied force of about 400N for which the piezoelectric element has given a current of 2.34 mA and voltage of 5.40 V as it is seen from Figure 11.

3.2 Characteristics Analysis Simulation of Piezo Material:

The burgeoning of immensely low power electronics has prompted an immense sense of interest for energy harvesting through the development of small-scale generators. Generally, these piezo-materials have mostly been applied to power sensors and wireless communication systems so far. The study shows how a piezoelectric bimorph can be developed to produce electrical energy under varying frequency, electric load and acceleration. To account for that the piezo sensor (PZT) is placed on a system that continuously produce vibration under a sophisticated design. The overall energy producing system that has been developed in the following design comprises of a bimorph having piezoelectric characteristics. It is attached at one edge of the vibration generator with a solid structure adjusted on the other edge.

Initially, the output power is observed as a function of oscillation having a constant load resistance connected to it. Secondly, the output power was analyzed with respect to a varying electrical load. Lastly, the positive output voltage is shown with respect to varying acceleration as well as the generation of sinusoidal voltage under a harmonic load as a function of time.

Simulation:

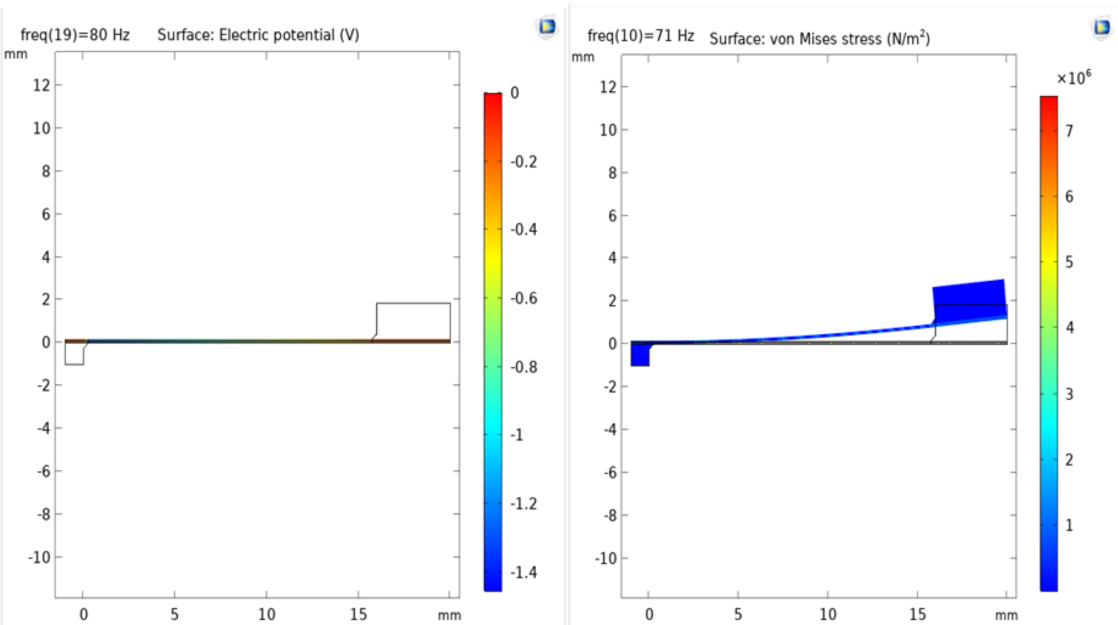

Figure 12: Energy Harvester under varying stress (a function of frequency)

Figure 12 explains the overall geometry of the model. The piezoelectric model is designed with a ground plane integrated with the neutral surface of the support. Moreover, the positive conductive planes are joint together on the outer surfaces of the piezoelectric structure. It makes sure that identical voltage has been induced throughout the outer surface of the conductive plane, nevertheless the pressure exerted on top and bottom of the ground plane is reverse in direction. Since the structure is attached to a vibration generator, it allowed the system to be examined under an oscillating framework.

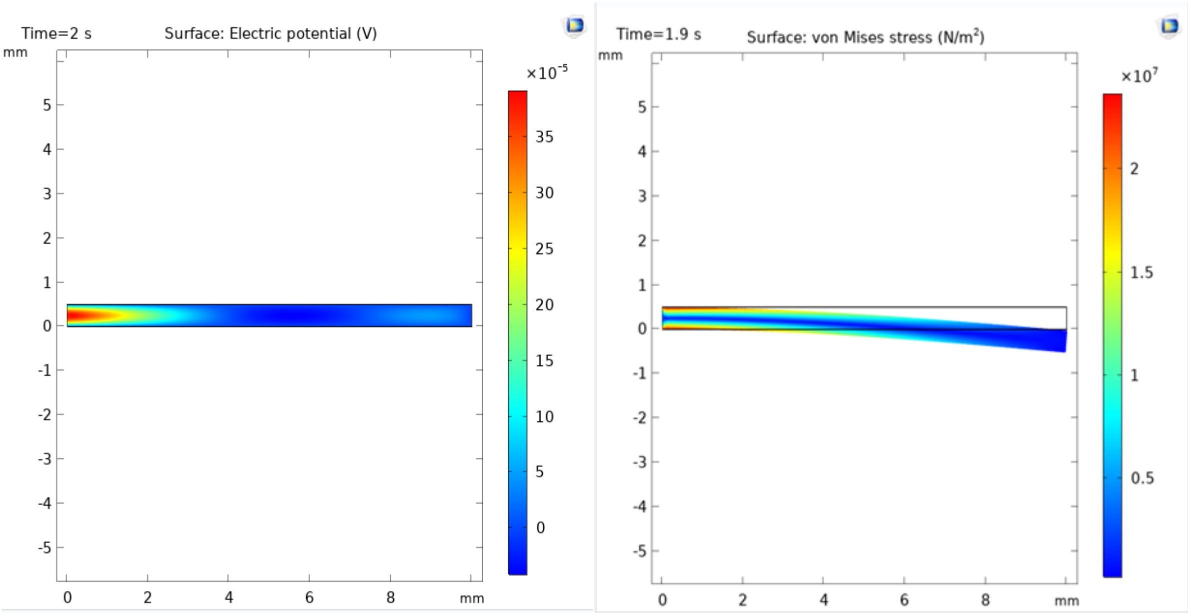

Figure 13: Energy Harvester under varying stress (a function of time)

In Figure 13, we demonstrate how the piezo-material reacts to a harmonic load and observe the generated output voltage due to harmonic oscillation.

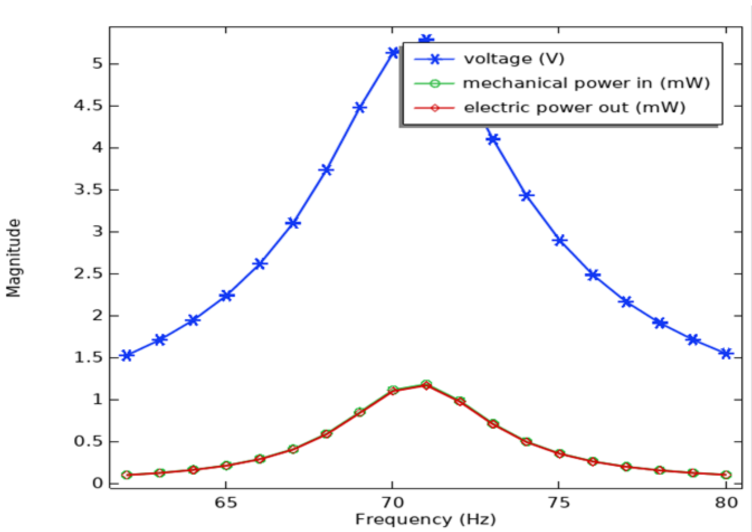

Figure 14: Relationship of input mechanical power, the electric power (in mW) and the maximum induced voltage across the piezoelectric block (in V) as a function of frequency.

Figure 14 represents the input mechanical power, the converted electric power (in mW). Moreover, it shows the maximum positive induced voltage throughout the conductive part of the piezo structure as a function of varying frequency. During this period, the piezo-material was stimulated through a harmonic acceleration. From the simulation result, we can approximate that the response of the system shows a peak at 70.5Hz that is the resonant frequency of the model. It explains that the mechanical power, electric power and induced voltage gradually increases along with frequency until the resonant frequency is reached.

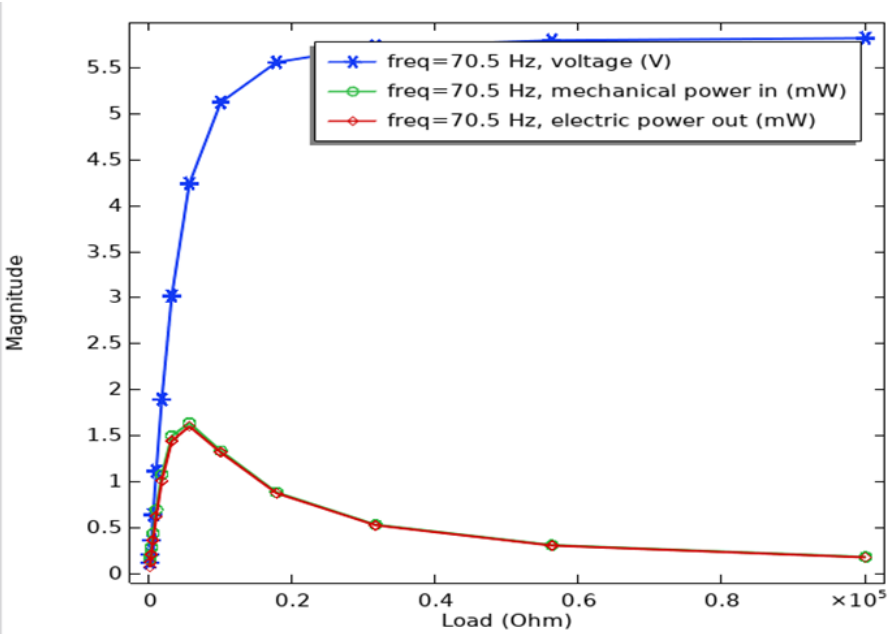

Figure 15: Relationship of input mechanical power, electric power and induced voltage with respect to a varying load resistance with a constant acceleration of 9.81ms^(-1) and oscillation at 70.5Hz.

Figure 15 demonstrates how the electrical power and induced voltage across the positive electrode of piezo-electric beam changes with respect to the varying load resistance under a constant acceleration of 1 g and frequency at 70.5Hz.

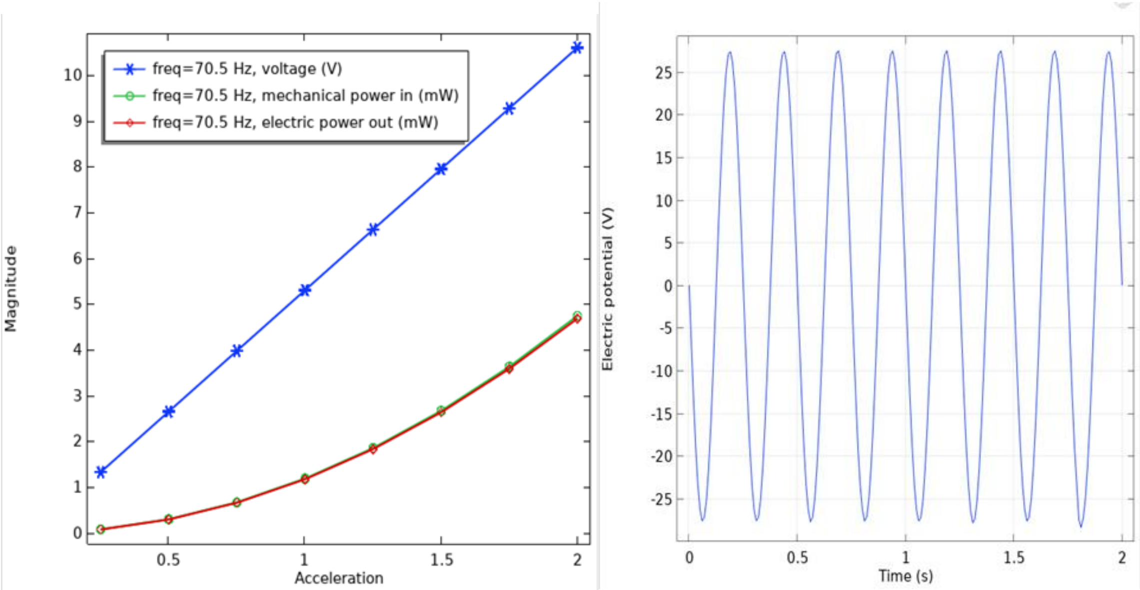

Figure 16: Relationship of positive induced voltage on the electrodes, electric power and mechanical power as a function of acceleration (g) and the sinusoidal output voltage under a harmonic load as with respect to time.

Figure 16 represents the voltage increases linearly under a fixed load, while the harvested power increases quadratically, as shown in equation (IV) [26]. It also explains that we can further increase the induced voltage and electric power of the design beyond the rated value for its earlier resonant frequency just through increasing the acceleration. This is to mention that these results completely comply with the findings in [26]. On the other hand, the other part of the simulation result represents the generation of a sinusoidal voltage output under a harmonic 12Ω load, but this representation might vary in practical circumstances, as it is difficult to maintain a harmonic pressure exertion in real life application.

3.3 Energy Generation from Solar Panel

The main function of the Solar panels converting light into electricity. Scientists often refers solar panels as photovoltaics which basically means "light-electricity." Enough power can be generated with distributed arrangement of many small cells across the broader area of panel, which in turn produces electricity [6].

Photovoltaic (PV) panels acquire energy from the sun to produce electricity. A PV panel consists of many solar cells in series connection so that we have the sum of all the voltages as the output. Each solar cell consists of 3 layers of which 2 layers are p type material and n type material of the semiconductor. The p and n type materials are joined together in order to form a pn-junction. The p type semiconductor has hole as majority carriers and electron as minority carriers; the n type semiconductor has majority electron carriers and minority hole carriers. Due to differences in concentration holes and electrons, the hole present in the p type material gets diffused with n type material and those electrons present in the n type material gets diffused with a p type material. As a result, electron hole pair recombination occurs and the negative ion near the junction of p type material and the positive ion near the n type material is exposed. This layer of negative and positive ions near the junction is known as the depletion region. The sunlight easily penetrates the top thin layer of the solar cell and causes the photons from the sunlight to reach the depletion layer and knock off the electrons from the neutral atoms. This produces a free charge carrier. Then the electron moves towards the n type material and consequently, the hole moves towards the p type material for the presence of the intrinsic electric field causing the production of electricity.

The radiation from the sun reaches the cells of the panel that turn goes to the Charge controller being transformed. Besides, the load is also connected to the controller. As the DC load, sunlight contacts with the solar cell modules, it starts to convert solar irradiance into DC electrical power that directs towards the charge controller. The charge controller maintains the level of amperage and voltage which gets delivered to the loads and the extra generated power goes to the battery system where batteries avoid conditions for not getting overly charged [27].

Calculation of Solar Panel Size, Controller and Battery Specifications

The following calculations of different parameters help to determine the suitable panel size, battery capacity and controller specifications required to drive the load.

1) First, we need to calculate the desired electricity power (in Watt) in order to drive the Air Water Generation System.

From the on-grid supply, we determined that

Supply voltage, V = 12V;

Supply current, I = 2.35Amp;

So, the power consumption is approximately P = VI or P = (12 * 2.35) W;

We get, P = 28.2 W

$$\text{Battery Size (A-H)} = \frac{Total\ Power\ (W) * Operational\ Hour(H)}{Battery\ Voltage(V)} \qquad (3)$$

$$= \frac{28.2W * 12H}{12V}$$

$$= 28.2\ A - H$$

Now, we can easily determine the Watt-hours value of the solar panel in order to drive a 28.2-watt load for 8 hours, simply through multiplying the load power with its operating hours.

It would be = $28.2\ Watt\ \times 8\ hours = 225.6\ Watt - hours$

So, the panel must meet the requirement to drive the load for 8 hours. However, it is a matter of fact that the peak sun hours duration is 7-10 hours during summer from the perspective of Bangladesh as seen from SWERA Bangladesh Report [28]. On the other hand, during the winter season we usually get 4-5 hours of suitable sunshine [28] that is very crucial in determining the panel size. Analyzing the peak sun hours of both summer and winter, we can reach to a conclusion that we must calculate the solar panel size considering the effective sunshine of winter season so that our load operates under optimal power supply throughout the whole year.

To account for that we will consider only 4.5 hours of suitable sunshine on an average day of winter. In doing so, we can ensure that the load is being supplied with the optimal power throughout the whole year.

$$\text{Solar Panel Size} = \frac{W-h}{Peak\ Sun\ Hour * Over\ Size\ Factor * Dust\ Factor} \tag{4}$$

$$= \frac{225.6\ W-h}{4.5H * 0.9 * 0.9}$$

$$\cong 60W$$

Battery Ah Calculation:

As of now, we are done with the calculation of the required solar panel size to drive the load during winter season. In this section, we will proceed with the calculation of required Ah rating of the DC battery that will supply to the load during solar intermittency and low solar irradiance to ensure sufficient power to the AWG system. We are using a deep cycle lead acid battery. One of the defining traits of deep cycle battery is that it can discharge up to 80% [29], which can be a major advantage for us, yet it was discouraged to discharge the battery below 45% on a regular basis as it might reduce the lifespan of the battery. As the rated voltage of our deep cycle lead acid battery is 12V, therefore in order to run the load for 12 hours at a stretch, the calculation would be:

By dividing (28.2*12) Watt-hours by the rated voltage, we can estimate that it will eventually require a battery having 28.2 A-h battery capacity.

Considering the depth of discharge of the lead acid battery to be 0.8,

We get, $$= \frac{Battery\ Size\ (A{-}H) * Autonomy\ day\ (1)}{Depth\ of\ discharge\ (0.8)} \tag{5}$$

$$= \frac{28.2(A{-}H) * 1}{0.8}$$

= 35 A-H $\cong 30\ A - H\ (approx.)$

Solar panel required to charge a 30Ah battery:

A solar panel with (12V-100W) rating defines the instantaneous rating of the panel. Therefore, under suitable testing conditions, the output voltage of the panel is supposed to be around 15-18 volts. As we know DC power is equivalent to voltage multiplied by current, we can approximate that current amperage level will be around the range of 5.5-6.6 amperes, ($\frac{100\ Watts}{18\ Volts}$ /$\frac{100Watts}{15Volts}$) from the panel. Therefore, we can estimate that a 100W panel can provide us 5.5 amperes per hour [30].

We can approximate that we can get around (5.5 Amp ×4.5 Hours) or 25 ampere-hours per day from a 100W panel on an average sunny day during winter season for a peak sun hours of 4.5 hours). This means we would need a 100-watt solar panel to charge our 30A-h battery completely on an average sunny day during winter [30].

Solar panel required to drive the load and to charge a 30Ah battery:

Based on the earlier calculation, we can estimate the required PV panel size on an average sunny day during winter season for a peak sun hour of 4.5 hours = 60Watt + 100Watt = 160 Watt. Normally, this reading is needed for winter. Since we did our experiments in relatively summer time, the 65W solar panel (Figure 17) was sufficient to supply required voltage and current to our system. Hence, a 65W solar panel is being used to supply power to the AWG system as well as the DC battery with the help of a (12V-6A) charge controller (Figure 19).

Figure 17: 65W-12V Solar Polycrystalline Solar

This is to mention that we cannot directly connect our panel with the load since there will be high fluctuations in the initial PV power. To account for that we would require a charge controller which constantly sense the PV output power and regulate it to the suitable operating voltage of the battery and load. It's a very crucial part of the solar power generation system. It safeguards the battery from overcharging and prevents possible overheating phenomena in load that might occur due to high voltage supply.

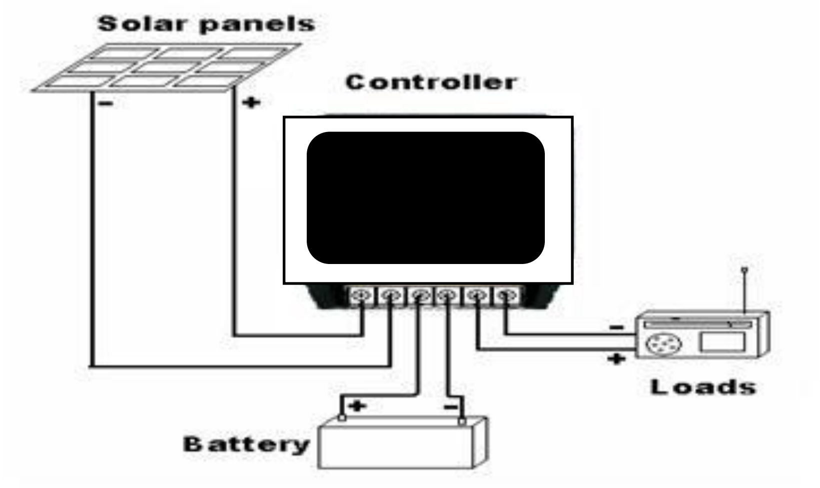

Figure 18: Solar Panel and Charge Controller Wiring Diagram

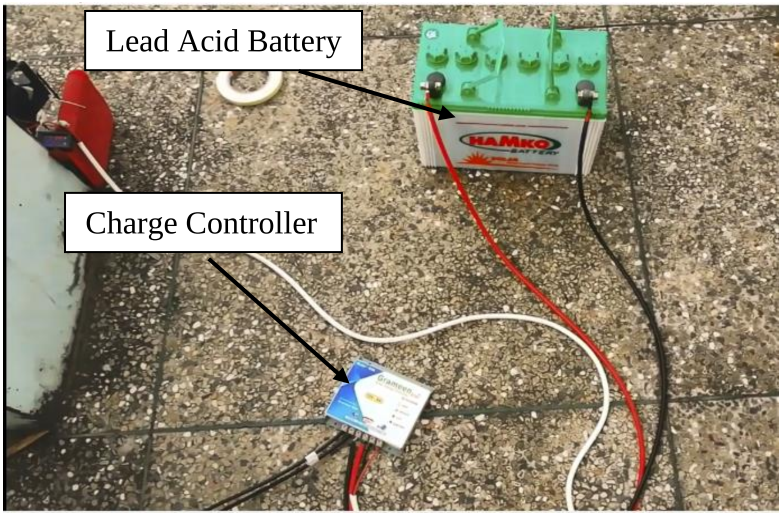

Figure 19: 12v-6A Charge controller, Battery and Load connection

Wiring steps of the Solar Panel and Power Generation:

To be very specific, there are mainly four steps in the wiring process the solar power systems as shown in the schematic diagram of Figure 18-

Step 1: Connecting the battery – To avoid short circuit and fire hazards, we should carefully deal with positive and negative ends of wires going to the battery and charge controller. The battery needs to be connected or disconnected first as it gives power to the charge controller.

Other parts, that is PV panel and load should be connected with controller after the battery connection.

Step 2: Connecting the load – It is to be ensured that the rated voltage of the battery should be in harmony with the load requirement. Positive and negative ends of load will go to the indicated ends as per the controller configuration. Fuse can be incorporated to avoid unwanted short circuit on the load side.

Step 3: Connecting the PV array – Photovoltaic arrays can cause very high voltages. Therefore, we have to be careful while wiring the panel to avoid electric shock.

Step 4: Checking the connection – Finally, we should recheck connections of each component whether they are properly connected and tightened or not.

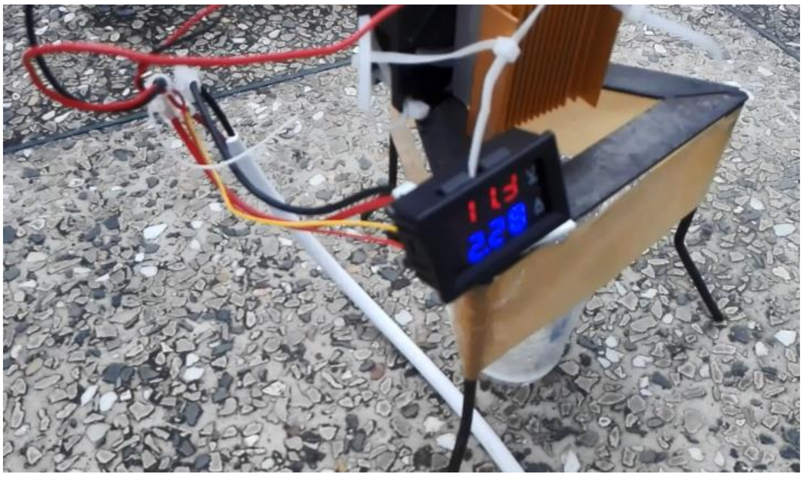

Figure 20: Digital Voltmeter-Ammeter reading across load

For convenience a Digital Voltmeter-Ammeter is incorporated with system as it is seen from Figure 20. The contribution from Piezo is utilized in this part of the project.

3.4 Complete Model Prototype

Figure 21 demonstrates the complete setup which were done for the field test. The solar PV panel, the AWG system (Load) and the lead acid battery is connected to the charge controller. Again, the Piezo materials mounted on the tiles lights up the display and shows how much voltage and current is passing through the load. Whenever, someone walks on the tiles, with the stress mechanism it produces the voltage and current. Rectifiers, capacitors and Diode are incorporated in a circuit for maintaining direction of the flow of voltage. And the main power for running the AWG comes from the solar panel depending on solar irradiance.

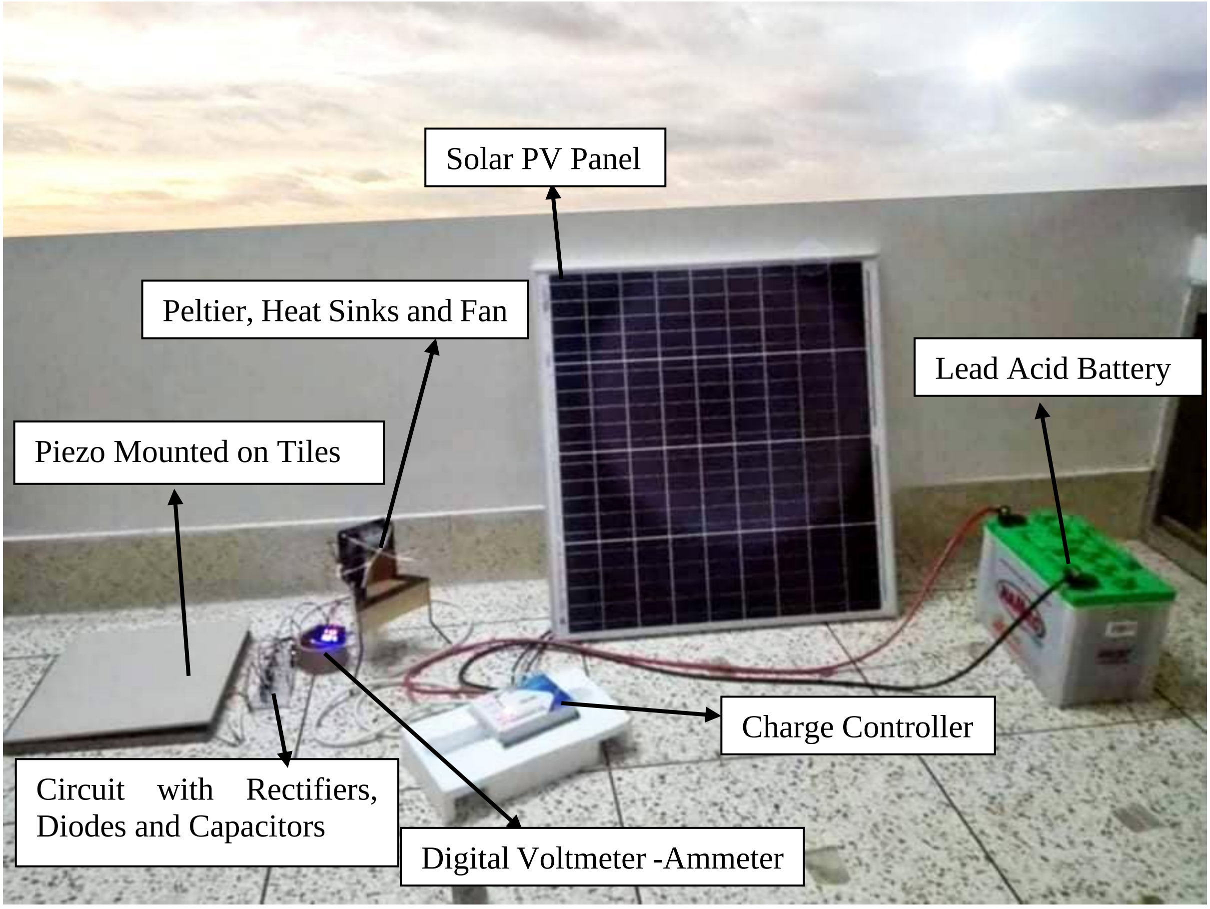

Figure 21: Design Parts of the Hardware Prototype

3.5 Result Analysis of Produced Electricity

For Piezo part:

The approximate weight that will be experienced by the piezoelectric element mounted under the tile every time a person walks on it will be around 80 kg. Our piezoelectric ceramic has a diameter of 35mm. Therefore, the induced mechanical stress (σ) will be:

σ = Force or area of each of the ceramic plate

σ= 80*9.81/ (π * (35*10-3/2)2)

σ = 815704.812 N/m2

Charge Density = Piezoelectric strain coefficient (d33) * σ (6)

= 390 * 10-12 * 815704.812 = 3.181 * 10-4 N/Vm

Each plate charge = Density of Charge * Area of the single plate (7)

= 3.181 * 10-4 * (π * (35*10-3/2)2) =3.06*10-7Nm/V

Open Circuit Voltage = Piezoelectric Voltage Coefficient * σ *t (8)

= 24*10-3 * 815704.812 * 0.002 = 39.2V

This value is close to the practical value.

For Solar part:

From our practical experiment, voltages are taken across load, PV panel and battery at different instances and an average value is considered,

Load Voltage = 11.3V

Load Current = 2.28Amp

We have experienced slight fluctuations in the output voltage and current due to varying solar irradiance level. The voltage level oscillated within the range of 11.2V to 12.7V and the current amperage level from 2.2 Amp to 2.6 Amp throughout its operating hours. However, these fluctuations did not create any noticeable impact on the load. The AWG system ran smoothly throughout its six hours of operation.

Chapter 4

Atmospheric Water Generation

4.1 Working Principle of Peltier Device

The water generation will be made to occur by the condensation of the humid air by the phenomenon of Peltier effect seen in the Peltier device. The two faces of the Peltier module are the two thermo coupled junctions. The junction is connection with the positive source end is where the holes and electrons are flowing. As a result, creating a potential difference across the junction that causes the junction to absorb thermal energy (cooling effect) to balance the difference in the chemical potential of the two materials. Simultaneously, the junction connected to the negative terminal undergoes an opposite effect and becomes hot [31].

Two Aluminum heat sinks will be attached on the two faces of the Peltier module. In addition, a DC exhaust fan will be brought into the scene for rejecting heat from the hot surface of the Peltier module. The heat sink placed on the hot side will be attached to ease the heat rejection process and the heat sink on that of the cold side will aid the condensation process as the distance between the water vapor particles will be reduced and the rate of collisions of the particles will increase due to the increase in the surface area. Both the exhaust fan and the Peltier module will be connected to the DC source (Rechargeable Battery) in parallel. Finally, a beaker will be left under for the extraction of the condensed water.

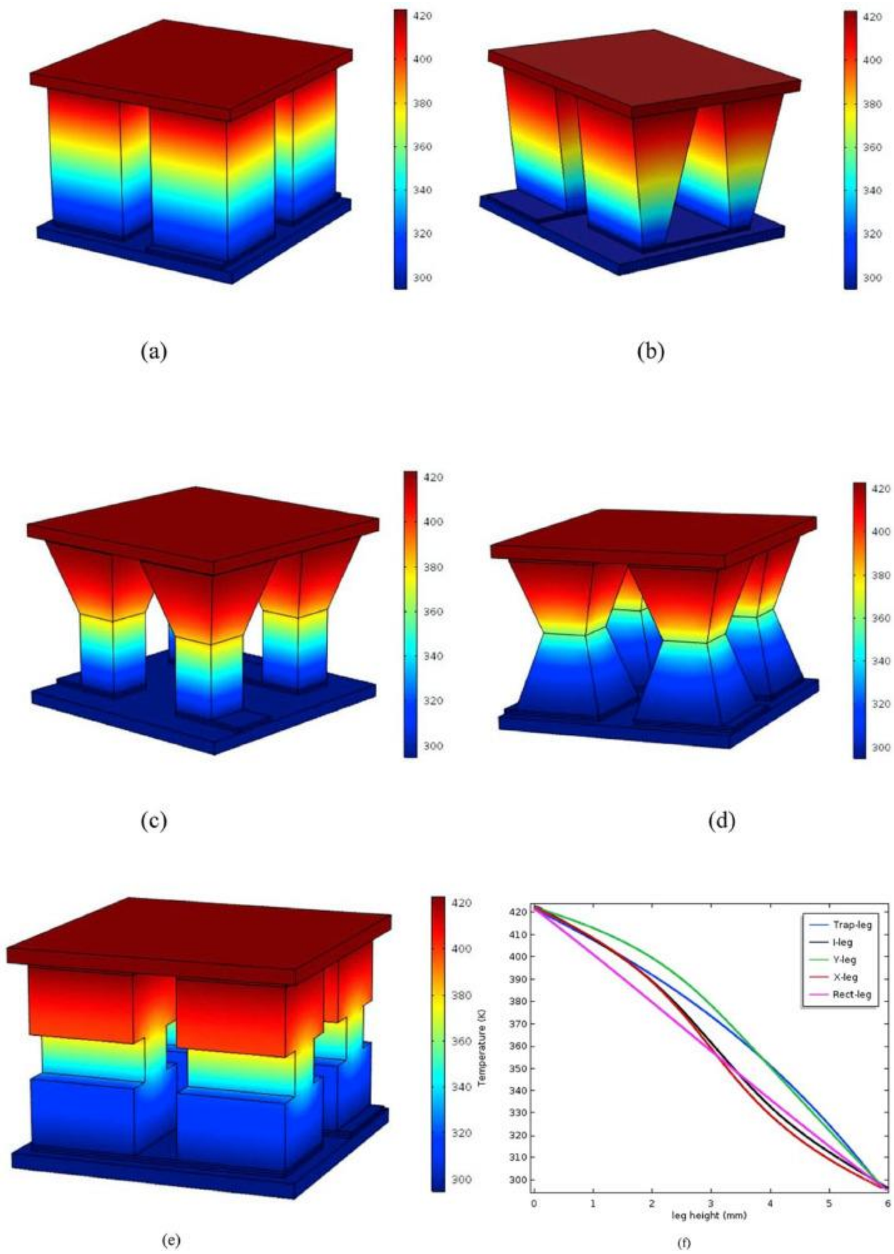

Figure 22: Simulation result of temperature variation of hot and cold side of Peltier device [32]

The above-mentioned simulation result in Figure 22 refers how the temperature varies between the hot and cool side of the Peltier module with a varying current level. From this data, we can interpret that the higher the current flow across the Peltier device, the more the temperature difference therein. It is evident that if we apply a high current up to the rated current through the device, then the module achieves the temperature to oversaturate and to condensate the cool side region rapidly.

4.2 Procedures in Efficiency Management

For ensuring the maximum water efficiency, we did continuous test through discussion of available knowledges acquired through research papers, personal experience and putting learned theories in action. First modification we brought is using container with very small surface to reduce the rate of evaporation from the container. Moreover, having the container closed prevented the water loss from the container. In this way, the water that was accumulated was averted from escaping in the form of water vapor.

Furthermore, we noticed that the surface of the Peltier was a plain and a uniform surface which made the condensed water that was formed on the surface more prone to experience evaporation. In order to tackle, the consumed water attached to body of the Peltier, we tried to increase the surface area of Peltier and below used a funnel cone-shaped wrapped with aluminum foil that helps for flowing of water faster.

4.3 Data Collection Mechanism

We measured the water consumed based on basis of water comparing with temperature and humidity. We did several tests, and in every test, changes were implemented for gaining the efficient results.

First three data tables are presented testing from on-grid supply and the following data are obtained. And some mechanical disadvantages are also present here as per initial designs and less water is consumed. In later cases, better equipment and modified design was incorporated which helped in increasing the efficiency of the Atmospheric Water Generator.

The last two tests are done under off-grid connection using solar panel, charge controller and battery. First 20W and small li-ion batteries were used. It had high discharge rate and power supply was very much inefficient. Later with 65W and Lead Acid Battery, the efficiency increased in the supply of electricity as well as modifications done with AWG also helped in giving better results. Below are the data tables of our different field tests along with mentioning the changes brought in the AWG system.

Initial condition: No fins used, open structure

Table 2: Day 1 (only with the prototype)

Time Passed	Temperature (Celsius)	Water Accumulated	Comments
1 hour	28	1 mL	
2 hours	29	2 mL	Evaporation affecting to lower water
3 hours	28	2.5 mL	
4 hours	27	3 mL	Increasing
5 hours	27	5 mL	
6 hours	26	5.5mL	Speed Decreased

Changes bought: Made semi closed around the Peltier

Table 3: Day 2 (Humidity and Temperature sensor incorporated and small container was used)

Time Passed	Humidity in Percentage	Temperature (Celsius)	Water Accumulated	Comments
1 hour	68	31	2.5 mL	Fast result then earlier
2 hours	69	31	4mL	Quick Progress
3 hours	71	31	7mL	
4 hours	70	31	8mL	Progress slowed
5 hours	70	31	9mL	
6 hours	72	31	9.5mL	Evaporation increasing

Changes bought: Used cone shape and aluminum foil

Table 4:Day 3 (Tried to make the whole system as closed as possible)

Time Passed	Humidity in Percentage	Temperature (Celsius)	Water Accumulated	Comments
1 hour	80	30	4 mL	Fast result then earlier
2 hours	80	30	4.5mL	Slower
3 hours	80	31	6.5mL	Relatively fast
4 hours	81	30	8mL	Progress slowed
5 hours	83	30	10mL	Better than last hour
6 hours	84	30	11 mL	Evaporation increasing

Changes bought: Used cone shape and aluminum foil, Fins, system unclosed

Table 5: Day 4 Test with modifications

Time Passed	Humidity in Percentage	Temperature (Celsius)	Water Accumulated	Comments
1 hour	83	31	4.8 mL	Better accumulation at surface
2 hours	84	30	10 mL	Slight faster
3 hours	83	31	13.8 mL	Slowed
4 hours	83	29	16.2 mL	Progress at constant rate
5 hours	84	30	19.5 mL	
6 hours	86	30	25.5 mL	Faster and better result

Changes bought: Used cone shape and aluminum foil, Fins, increased surface area of accumulation, made semi closed to reduce evaporation.

Table 6: Day 5 test (Complete Off grid Test) with modifications

Time Passed	Humidity in Percentage	Temperature (Celsius)	Water Accumulated	Comments
1 hour	83	31	25 mL	Increased area giving more accumulation
2 hours	83	31	38 mL	Rate is a bit slower hourly
3 hours	82	30	57 mL	Constant increased
4 hours	81	28	61 mL	Considerable slower
5 hours	84	28	82 mL	Rate increased
6 hours	83	29	99 mL	Nearly constant rate of increase

From a paper by Ruba Amarin [33] Saturated water vapor pressure at different temperature is shown based on some data collection.

Magnus Formula, which is an established approximation to determine the dew point T_{dp} is used here provided that the ambient ("dry bulb") temperature of the air (T°C) as well as the Relative Humidity (RH%) is known [33].

$$\gamma(T\ , RH) = \ln(\frac{RH}{100}) + \frac{bT}{c+T} \qquad (9)$$

$$T_{dp} = \frac{c\gamma(T,RH)}{b-\gamma(T,RH)} \qquad (10)$$

Several constant sets are in use in this context as for the value of b and c. David Bolton in his Monthly Weather Review Paper used the following [34].

Here,

- b is a constant and the value is 17.67,
- C is the temperature value which has been considered to be 243.5 °C

Sample Calculation:

$$\gamma = \ln\left(\frac{55}{100}\right) + \frac{17.67 * 33}{243.5 * \ 33} = 1.5068$$

$$T_{dp} \ = \ \frac{243.5*1.5068}{17.67-1.5068} = 22.7$$

Air Temp	30	31	32	33	34	35	36
RH (%)	**Dew Point Temperature (℃)**						
50	18.4	19.3	20.3	21.2	22.1	23	23.9
51	18.7	19.7	20.6	21.5	22.4	23.3	24.2
52	19.1	20	20.9	21.8	22.7	23.6	24.6
53	19.7	20.3	21.2	22.1	23	24	24.9
54	20	20.6	21.5	22.4	23.4	24.3	25.2
55	20.2	20.9	21.8	22.7	23.7	24.6	25.5

We know that,

Water partial pressure (Pw) = $\frac{RH\%}{100} \times P$ [33] (11)

Mixing Ratio at Saturation Level (W_s): W_s, (grams of vapor /kg's of air) =

$621.97 \times {P_{ws}}/{(p - \ P_{ws})}$ [33] (12)

Here,

P_w = Pressure of water vapor,

RH = Relative Humidity (RH%),

P_{ws} = water vapor pressure at saturation.

P = pressure of atmospheric air

Through humidity ratio, we get to know about the amount of water ($in\ m^3$) available within $1m^3$ of air.

We know it that,

$1m^3 = 1000L.$.

Therefore, we can write,

The maximal water (in L) available in $1m^3$ of air = $Humidity\ Ratio\ \times 1000$

Calculation:

Now,

For a given temperature (T) of 30°C and

Relative Humidity (RH) = 50% ,

Water vapor pressure at saturation (Pw) at 30°C

1mmHg = 0.00133322bar

so, 31.8mmHg = (31.8 * 0.00133322) = 0.04241bar [34]

(Data collected from saturated water vapor pressure table) [34]

Water vapor pressure at saturation, Pw = $\frac{50\%}{100} \times 0.0424 = 0.021bar$ [33]

HR (humidity ratio) = $0.622\ \times \frac{0.021205}{(1.0132-0.021205)} = 0.01329527$ [33]

the maximal water available in $1m^3$ of air = $Humidity\ Ratio\ \times 1000$

$= (0.01329527\ \times 1000)$

$= 13.29\ L\ (approx.)$ [33]

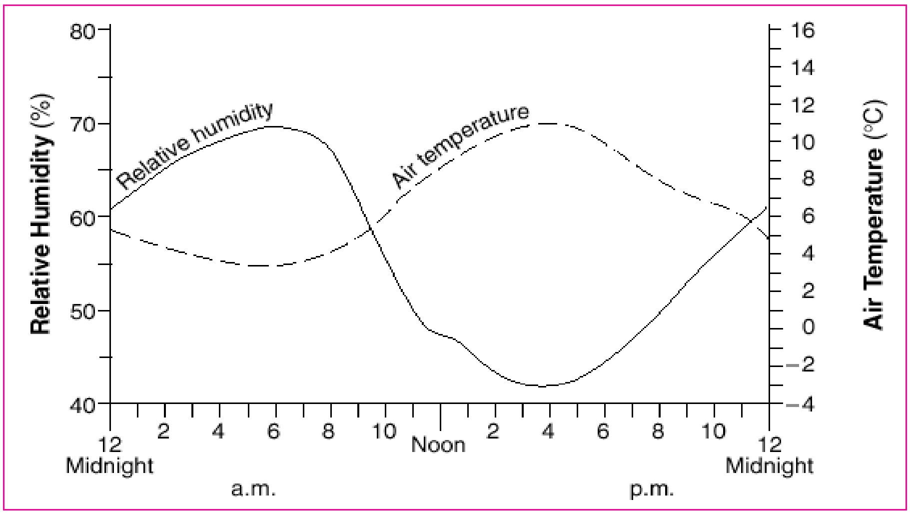

Figure 23: Relationship of Relative Humidity and Temperature [35]

From Figure 23, it can be inferred that relative humidity is inversely proportional to temperature. Furthermore, at a certain temperature when the relative humidity is high, the air particles near the cool side of the Peltier module reaches dew point temperature more rapidly even at a minimal deviation in temperature between the two plates of the module.

From the graph we can also interpret that, water extraction rate would be high between 12AM to 9AM and would be low 12PM to 10PM

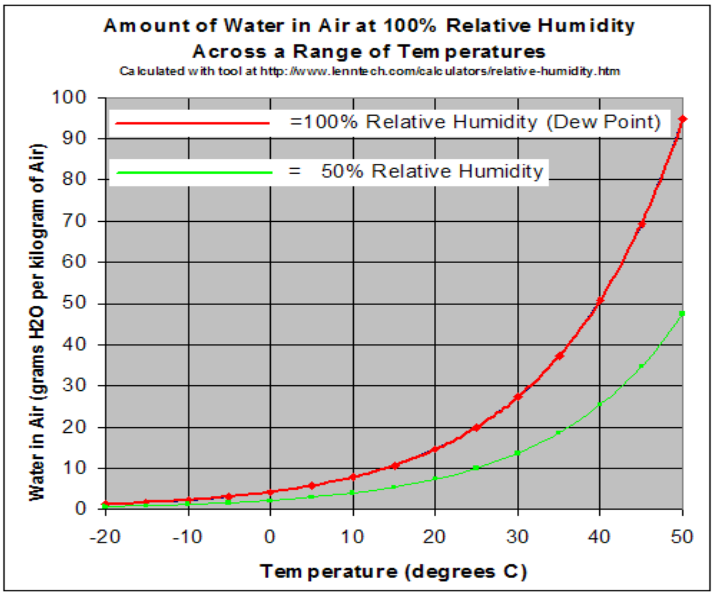

Figure 24: Amount of Water at 100% Relative Humidity [36]

The chart from Figure 24 displays the amount of water vapor that the air can hold goes up with an escalating temperature. The water vapor to air ratio (grams of water/kilogram of air) is referred to as the absolute humidity which is also known as the mixing ratio. The relative humidity is the percentage of the absolute humidity of the air with respect to the entire water vapor the air can accommodate at a certain ambient temp.

$$Relative\ Humidity\ (\emptyset) = \frac{Water\ Vapor\ present\ at\ a\ given\ temperature}{Max\ amount\ of\ water\ vapor\ air\ can\ hold\ at\ a\ given\ temp} \qquad (13)$$

Consequently, if the absolute humidity is 10 grams of water vapor per kilogram of air at 25 degrees Celsius(°C), we have a relative humidity of 50% or in other words the air is holding half the amount of water vapor it can hold.

To determine the saturated vapor pressure and the actual vapor pressure, the temperature must be converted to degree Celsius(℃).

Then, the saturated vapor pressure (e_s) and the actual vapor pressure (e) can be calculated using the formulas listed below [34]:

$$e = 6.11 \times 10^{\left(\frac{7.5 \times T_d}{237.3+ T_d}\right)} \qquad (14)$$

$$\text{And } e_s = 6.11 \times 10^{\left(\frac{7.5 \times T}{237.3+ T}\right)} \qquad (15)$$

In our latest experiment, we observed during the 1st hour:

The Ambient temperature (T) = 31℃

And the Dew-point temperature (T_d) = 27℃

Using the above-mentioned equation, we determined:

The actual vapor pressure (e) = 23.357 millibars (mb)

And the saturated vapor pressure (e_s) = 35.2959 millibars (mb)

We know,

$$\text{Relative Humidity (RH \%)} = \frac{e}{e_s} \times 100 \qquad (16)$$

$$= \frac{23.357\ mb}{35.2959\ mb} \times 100$$

$$= 66.17\%$$

4.4 Comparative Result Analysis of Consumed Water

A comparative analysis of water generation rate of Peltier module at different structural design:

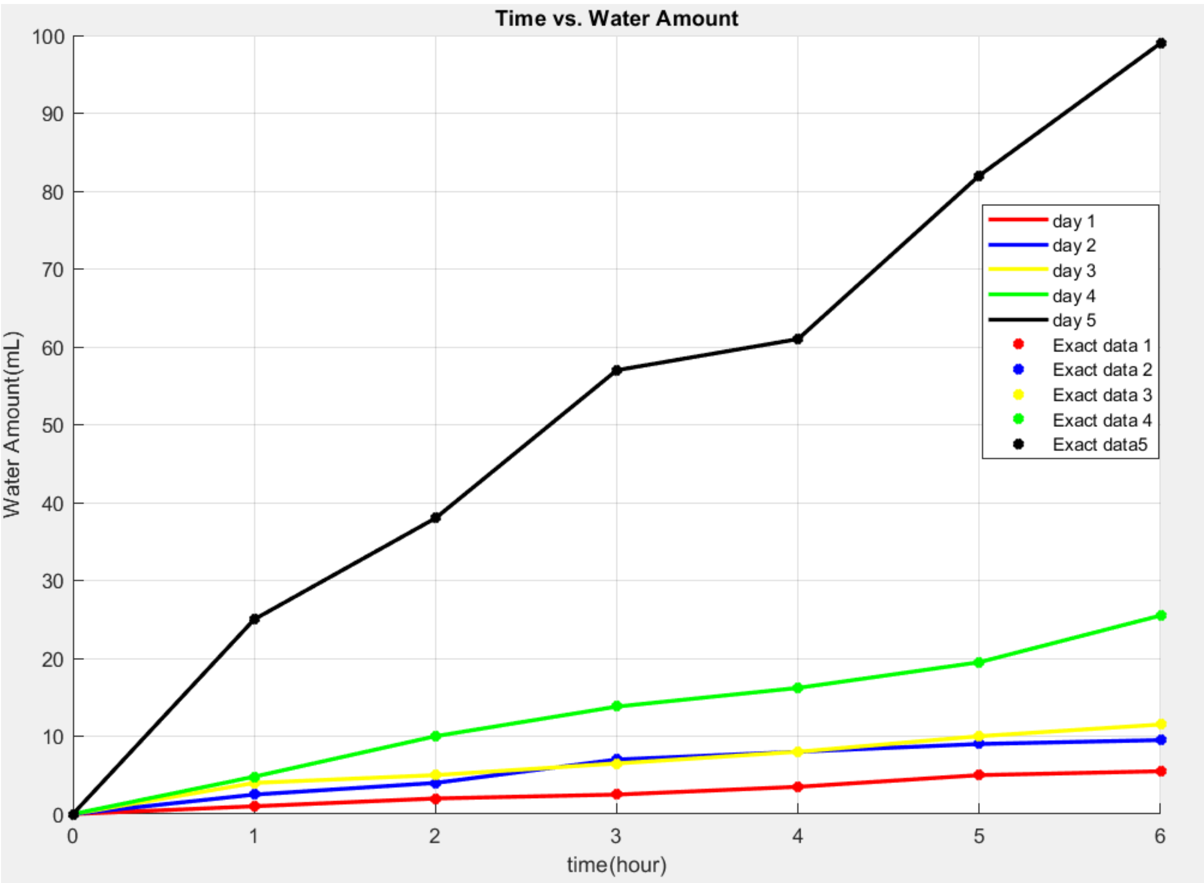

Figure 25: Comparative analysis of water generation rate of Peltier module from experimental data

Figure 25 shows the result analysis of our five-day field tests for the AWG system. With improvement in design and condition, changes in the water accumulation rate are observed. The humidity, surface area, surface tension and the impact of closed surface are being highlighted with the differences in data for our field tests.

Besides, we also compared our latest result with existing experiments done by other researchers for a clearer understanding of the efficiency rate.

Table 7: Comparison with Related Research of AWG system

Factors and Results	**Khadim's Study**	**Present Study**
Number of thermoelectric coolers (4cm*4cm)	1	1
Power consumption (W)	80	30
Relative Humidity (%)	65	65
Ambient Temperature (°C)	31	31
Air Velocity (m/s)	1	1
Material attached on the cool side of the TEC.	Aluminum cone structure of 6cm diameter and of 13cm height.	Aluminum heat sink (5cm*5cm) with rack like structure.
Temperature distribution on the material attached on the cool side of TEC.	Uneven distribution of temperature. The tip of cone is warmer than the base of the cone.	Relatively even distribution of temperature.
Water Generation Rate (ml/h)	10.1	25

Thualfaqir J. Kadhim et al [37] has attached a cone structure of 6cm diameter and of 13cm height made of aluminum on the cold side of the Peltier module in order to increase the surface area for having more accumulation of condensed water. However, it was elucidated that the cone structure was not really suitable for condensation purpose. The temperature across the cone structure was not uniform throughout the cone surface, which means that the temperature was not below the dew point on every portion of the aluminum surface. The surface was only cool enough for the portion, which was fairly near the cool side of the Peltier module but was warmer at the open-end portion. This uneven distribution of coolness on the surface made the water formed more susceptible to evaporation. Nevertheless, in our design, we have incorporated an additional aluminum heat sink of (5cm*5cm) dimension in direct contact with the cold side of the Peltier device that is of (4cm*4cm) dimension and the heat sink has a rack like structure on its surface. The temperature distribution is sufficiently even and all the portion of the structure has temperature lower than the dew point to carryout condensation and prevent rapid evaporation unlike the cone structure. Moreover, the heat sink on the cool side providing a rack like structure stopped the surface from being plane and prevented the evaporation to occur to a great extent. Furthermore, the heat sink integrated with the cool side of the Peltier module increased the surface that contributed to the condensation process substantially as the molecules near the surface encountered more collisions. Since the molecules near the cool surface lost kinetic energy and experienced more collision, the condensation rate was enhanced. Therefore, our design has solved the problem of uneven distribution of temperature; hence decreased evaporation rate and increased the condensation rate.

Thualfaqir J. Kadhim et al [37] study manifested that the Peltier module with an integrated heat sink on the hot side was placed horizontally, whereas, in our system, we sorted it in vertical position. In doing so, the thermoelectric cooler gets more exposure to cooler air, which adds fuel to the efficiency of the Air Water Generation System unlike the research of Kadhim et al [37].

Moreover, from the analysis of Kadhim [37], it was observed that the maximum water accumulation rate was 10.1mL/hr. from a single thermoelectric cooler at a relative humidity of 65% which differs from our findings in terms of the system performance as we were successful in collecting 25mL/hr. using one TEC, under similar environmental condition with respect to relative humidity level of 66%, air velocity (1ms^(-1)) and ambient temperature (31℃).

Last but not the least, another important aspect of the comparative analysis was to correlate our project with others in terms of power efficiency. Now, the work of Thualfaqir J. Kadhim et al [37] depicts that the AWG system comprised of one TEC and DC Fan consumed 70W to produce 10.5mL/hr. at a relative humidity level of 65% that required them to employ a 80W solar panel to support the power requirement, and in contrast to that our system having similar components with identical specifications only consumed 30W to produce 25ml/hr. under the same atmospheric condition. The system was powered by a 65W solar panel with a small contribution from piezo materials to drive a digital voltmeter-ammeter display that constantly shows the voltage and current level across the load. Therefore, from the above relative power efficiency analysis, we can conclude that our AWG system is more budget friendly and power efficient.

Chapter 5

MATLAB Simulation and Results

5.1 Complete System Representation with Solar PV Panel

In this simulation, we have integrated battery with the solar panel after taking the battery and solar controller unit and SWERA data into our conscious consideration [28]. We have used a 160W panel of 36 cells (4*9) considering 4.5 hours of effective sunshine on an average day of winter to supply to the load as well as the battery. Moreover, we have used a deep cycle lead acid battery of 30A-h to supply to the load during solar intermittency. The solar panel size and battery A-h capacity has already been determined in earlier calculations for hardware implementation. Our objective is to drive the load components as well as to charge the battery with the solar panel during high solar irradiance, but we have noticed that there are high fluctuations in the initial PV voltage and current due to varying solar irradiance. To account for that, we have incorporated the Maximum Power Point Tracking algorithm in the system where the MPPT system constantly sense the output parameters of the PV panel and regulate it depending upon the load requirement.

Maximum Power Point Tracking Unit continuously inspects the initial voltage and current generated by the PV panel and constantly matches it to the voltage level of battery in order to adjust the PV voltage based on the battery rating in such a way that it becomes best suitable to charge up the battery. Moreover, we can also connect DC load to the panel once the MPPT system and Buck-Boost converter does the necessary adjustment to optimize the load supply.

We know that the MPPT system works efficiently under certain circumstances which have been mentioned below:

- Normally, PV modules work more efficiently when the temperature is low. The MPPT system performs very effectively to optimize the power output that is being supplied to the load under the low temperature weather condition.

- Whenever the MPPT system senses that the battery is in a low state of charge, it immediately extracts higher amount of current by adjusting the voltage to a suitable level and escalates the charging rate.

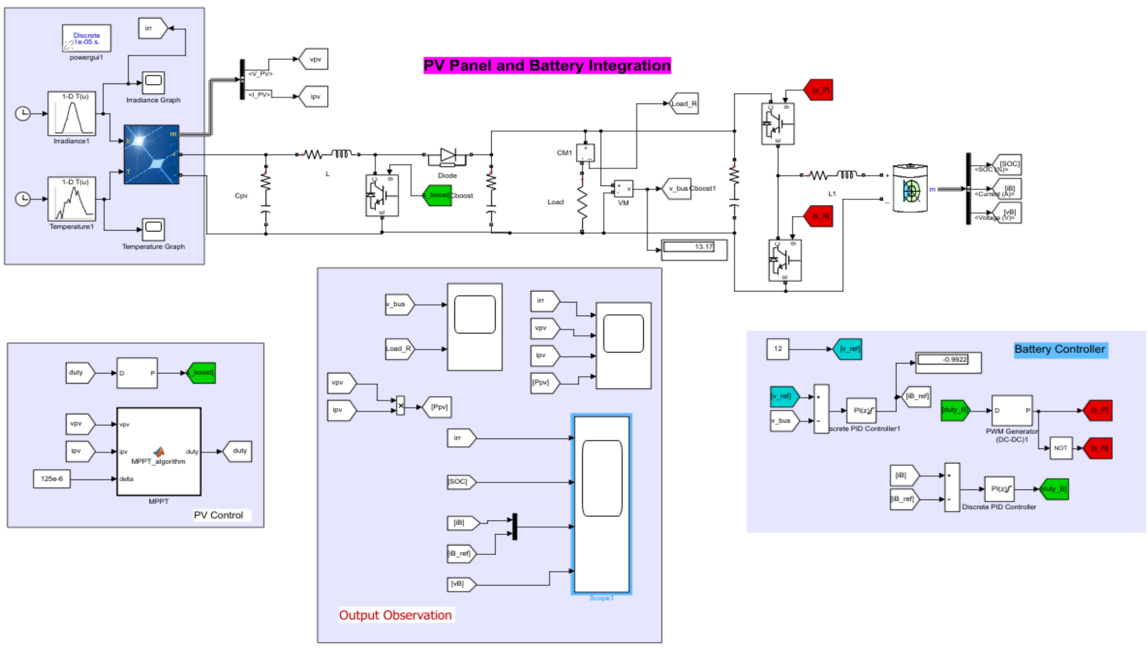

Figure 26: Integration of Solar Panel with Battery.

Moreover, we have employed a buck-boost converter associated with the MPPT controller which operates in harmony and maintains a constant of 12.5V (with +- 5% oscillation) as for the load voltage. The converter has the ability to change the duty cycle on its own by dint of the MPPT algorithm. Furthermore, the battery controller ensures an uninterrupted supply to the load during solar intermittency and low solar irradiance. Whenever the initial supply voltage and current from the PV panel falls below 12V and 2Amp respectively, the battery starts to discharge and provides continuous supply to the load. Figure 26 elaborates the complete design done through MATLAB simulation.

5.2 Specifications of Parameters for Solar Panel

According to 'The Solar and Wind Energy Resource Assessment (SWERA)' data report of Bangladesh [28], we have arranged the Global Horizontal Index value for a 24-hr. time format during the summer and the winter season.

- **SWERA DATA**

Solar Irradiance:

Table 8: Averaged Hourly GHI (Wh/m2) of August (Summer) [28]

Hours	5.30	6.30	7.30	8.30	9.30	10.30	11.30	12.30	13.30	14.30	15.30	16.30	17.30	18.30
GHI (Wh/m^2)	5	66	198	354	521	666	751	764	693	553	402	237	72	4

From table 8, we can estimate that there is 8 – 10 hours of effective sunshine during summer (August). Based on which we have to arrange the irradiance value in '1-D Look Up Table' block associated with the solar panel for summer (August).

Table 9: Averaged Hourly GHI (Wh/m2) of January (Winter) [28]

Hours	5.30	6.30	7.30	8.30	9.30	10.30	11.30	12.30	13.30	14.30	15.30	16.30	17.30	18.30
GHI (Wh/m^2)	0	3	57	175	300	411	494	518	483	379	236	94	10	2

Similarly, from table 9, we can estimate that there is 4-6 hours of effective sunshine during winter (January). Based on which we have to arrange the irradiance value in '1-D Look up Table' block associated with the solar panel for winter (January).

Note: 5:30 represents the period between 5am to 6am and so on.

MATLAB Plot of Solar Irradiance and Temperature Data:

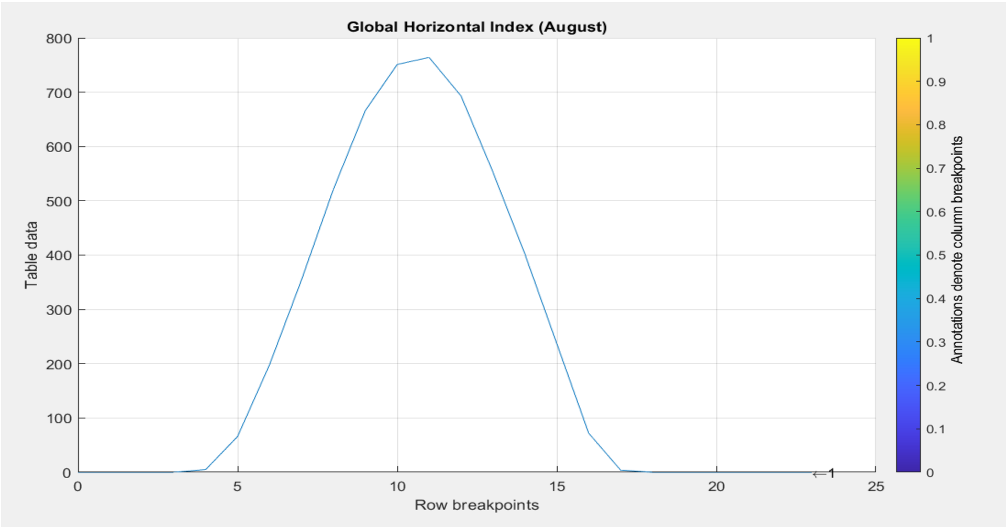

Figure 27: Average Daily GHI data of summer. (August)

In Figure 27, the MATLAB plot shows how the solar irradiance changes throughout the 24-hr. time format for a particular day in August.

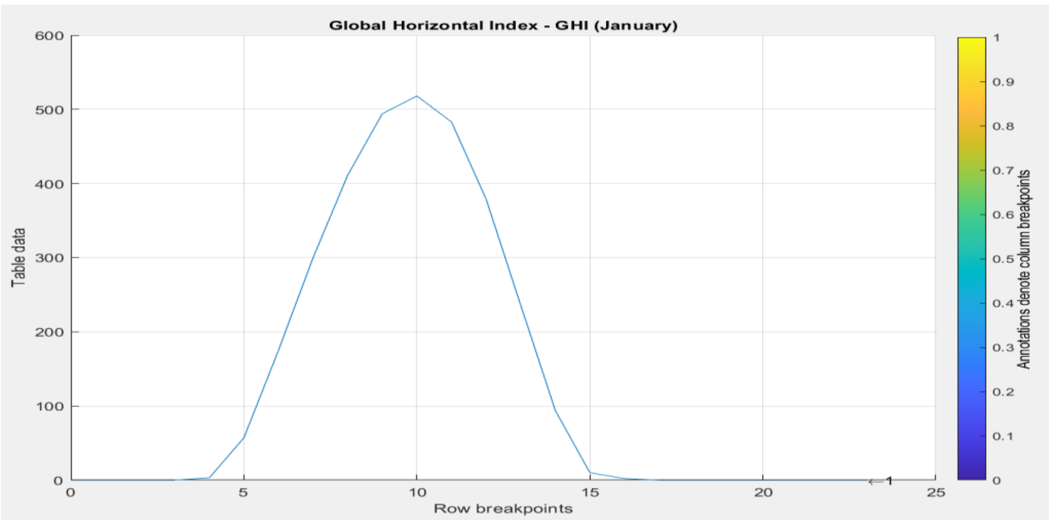

Figure 28: Average Daily GHI Data of Winter. (January)

Subsequently, in Figure 28, the MATLAB plot shows how the solar irradiance changes throughout the 24-hr. time format for a particular day in January.

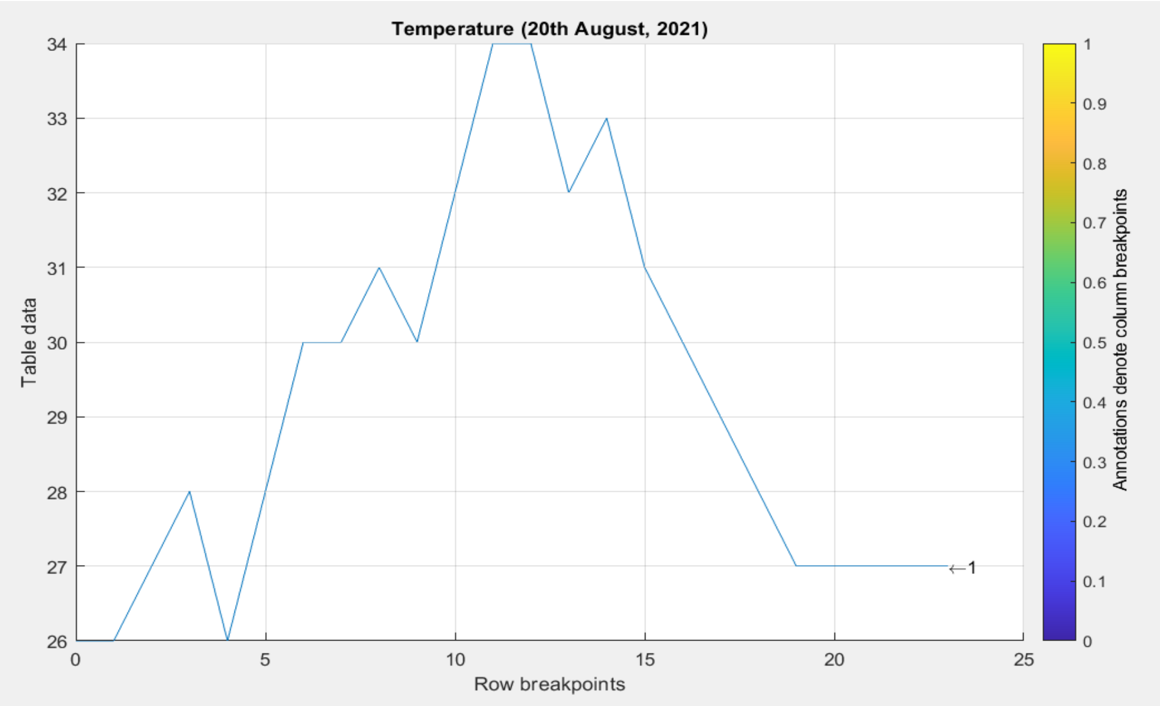

Figure 29: Average Daily Temperature Data of Summer (20th August, 2021) [38]

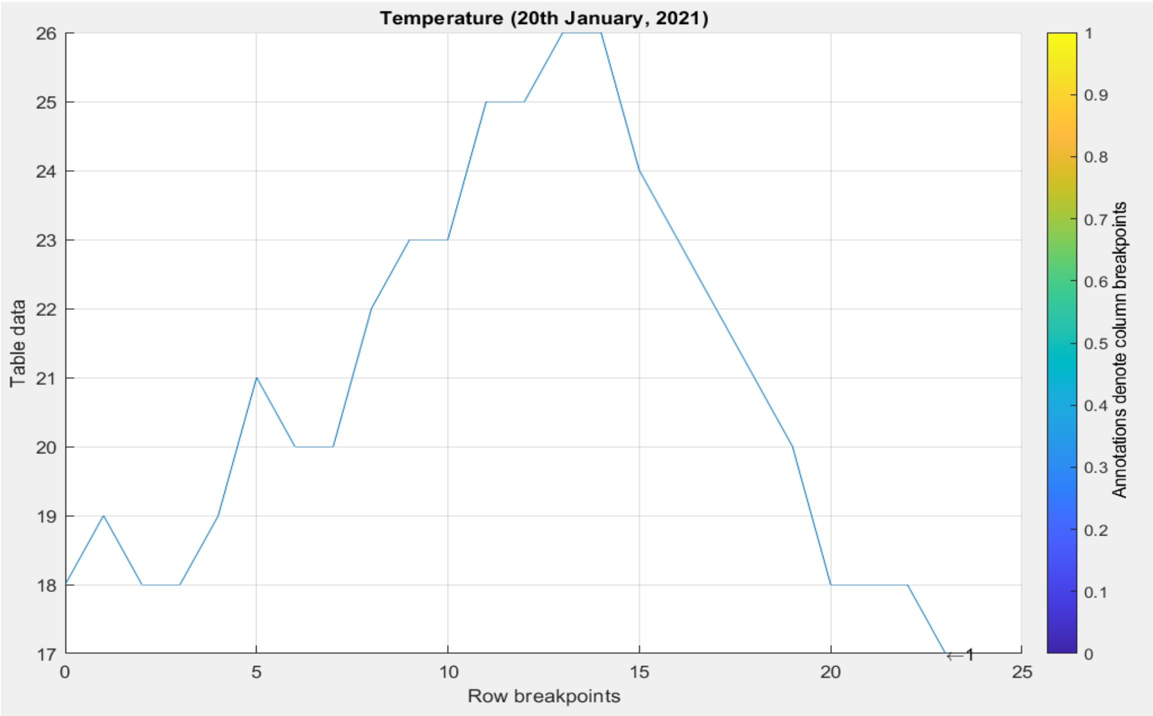

Figure 30: Average Daily Temperature Data of Winter (20th January, 2021) [38]

Figure 29 and Figure 30 refer to the average daily temperature data of August 2021 and January 2021 respectively.

5.3 Result Analysis PV Panel Simulation

i. Load current and load voltage

Figure 31 represents the voltage and current across the load, which has been maintained at a desired range in harmony with the rated voltage of the load components.

Here, load voltage = 12.5V (with +- 5% oscillation)

And load current = 2.4Amp. (with +- 5% oscillation)

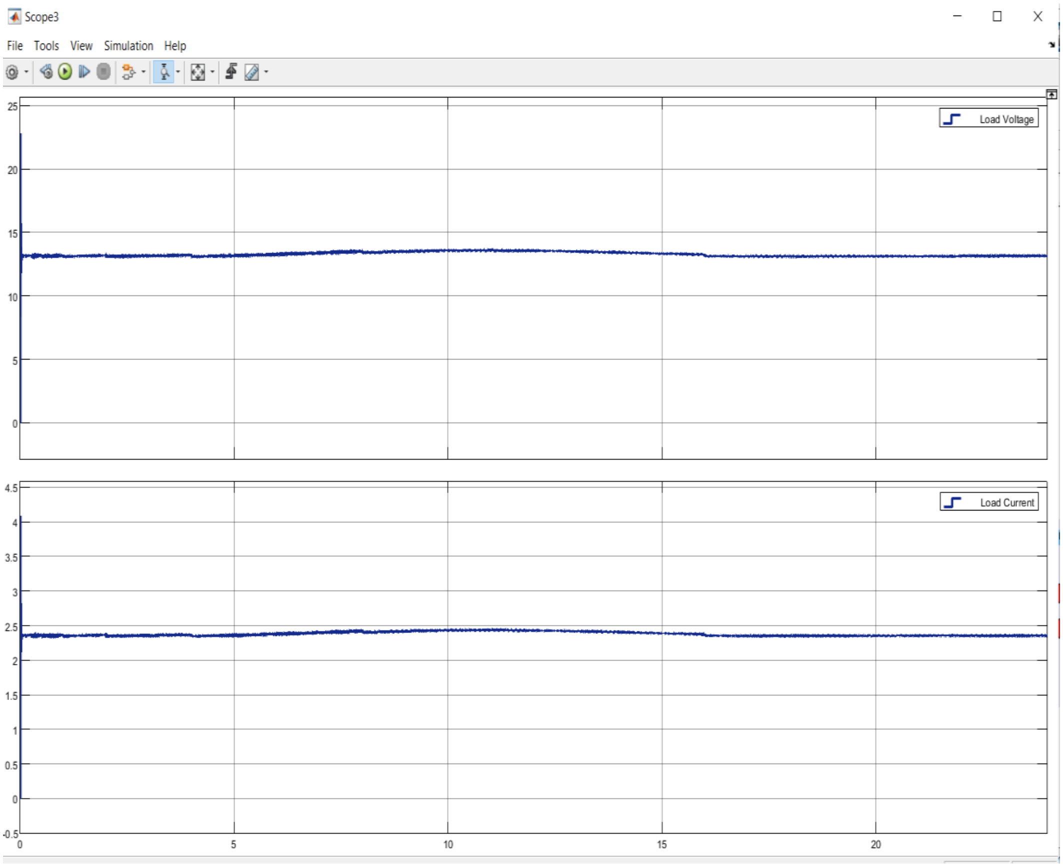

Figure 31: Load current and load voltage simulation

ii. Solar Panel Parameters:

Here, the solar irradiance values have been arranged based on an average sunny day of January, 2020 during the winter season. The maximum current and power that we could extract from a 160W solar panel during the peak sun hour is 8amp. and 115W respectively. Figure 32 shows how the PV voltage, PV current and PV power changes with respect to solar irradiance. The Solar parameters (V, I & P) are maintained at zero level during solar intermittency and start to increase as soon as the solar irradiance increases.

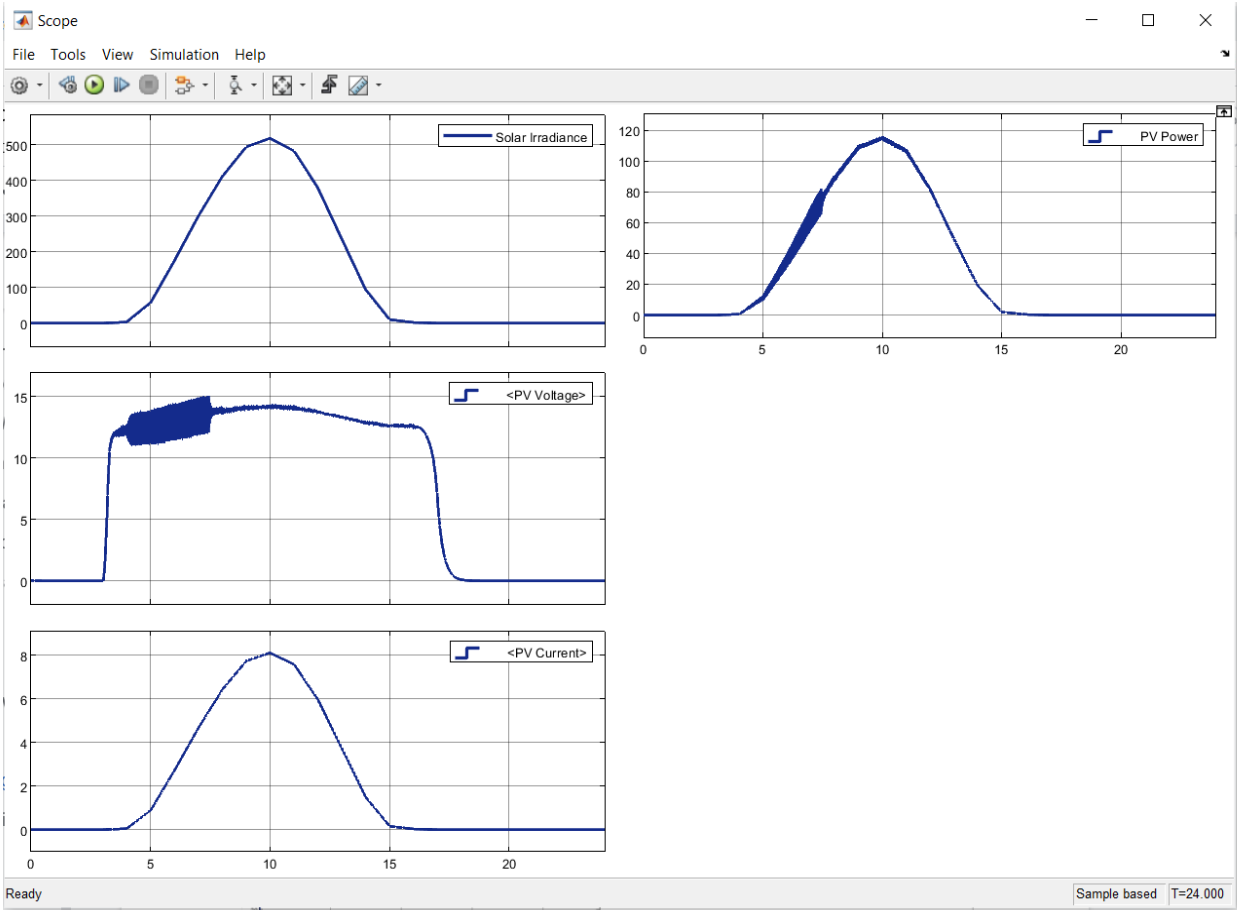

Figure 32: Solar Panel Parameters Simulation

iii. Battery parameters:

Specifications of the Battery:

Type of the Battery: Lead Acid Deep Cycle Battery

Battery Nominal Voltage: 12 Volts

Initial State of Charge: 60%

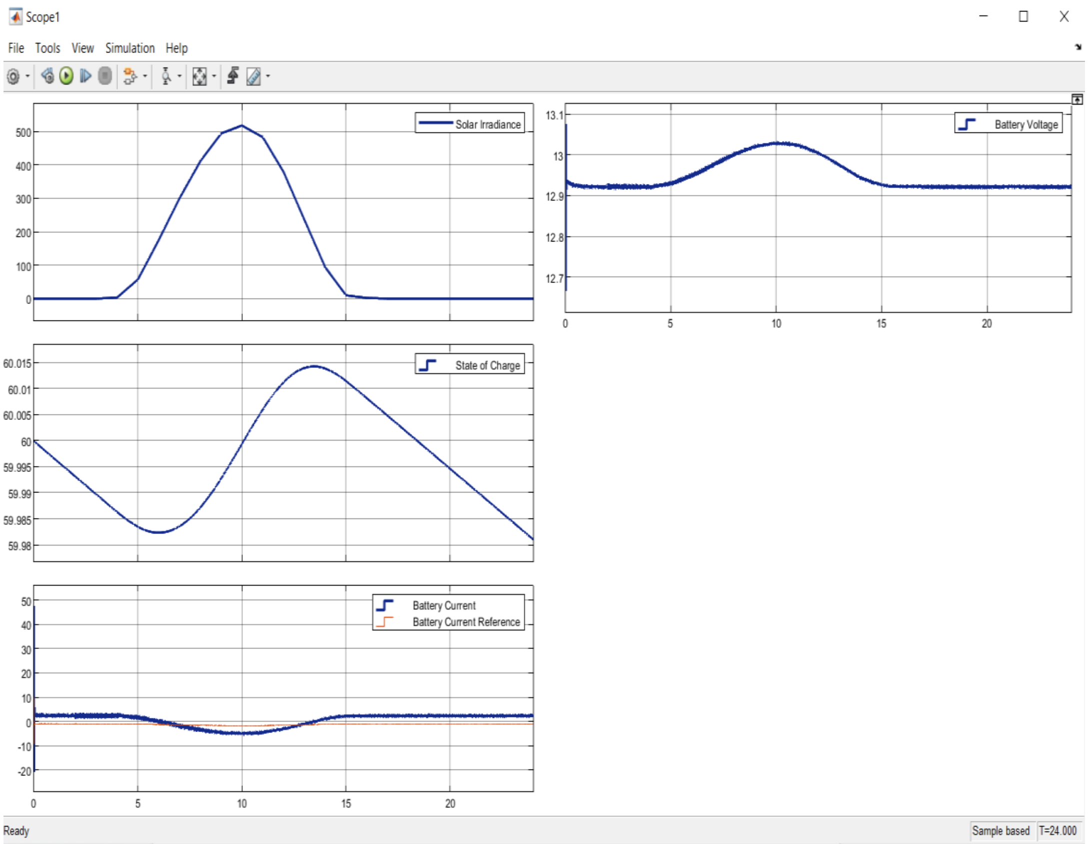

Figure 33: Battery parameters simulation

From the above-mentioned simulation result in Figure 33, we can observe that the battery is discharging during solar intermittency and low solar irradiance. As soon as the irradiance increases to a level that is sufficient to supply the load as well as the battery, the state of charge starts to increase and so does the battery voltage.

5.4 Relay based switching phenomena between battery and PV panel

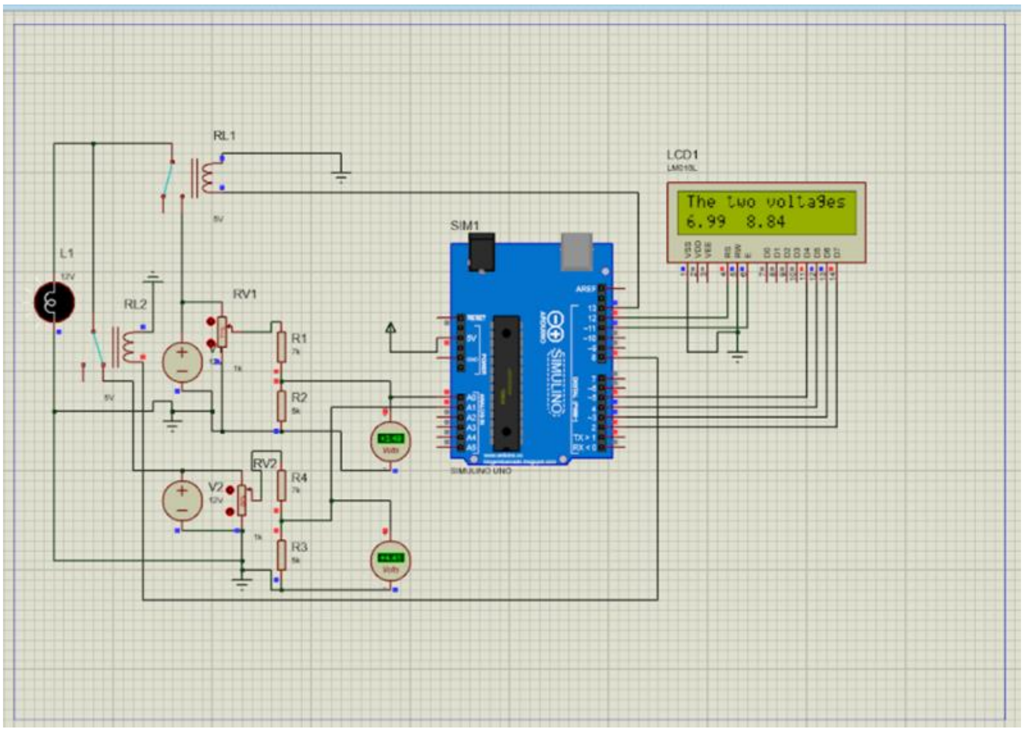

Figure 34: Relay switching circuit

The circuit shown in Figure 34 was used to test the code for the relay switch so it can be used for the relay switching phenomenon between the Solar Panel and the Battery. When the voltage from the PV panel is below 12V due to low irradiance, the load will get its power from the battery. The two voltage sources depicted in the Proteus circuit diagram are analogous to the two sources (PV panel and the battery) by which the AWG will be powered. The Arduino will compare the voltage level and turn the corresponding switches on and off.

5.5 Piezo Voltage and Current Generation Simulation

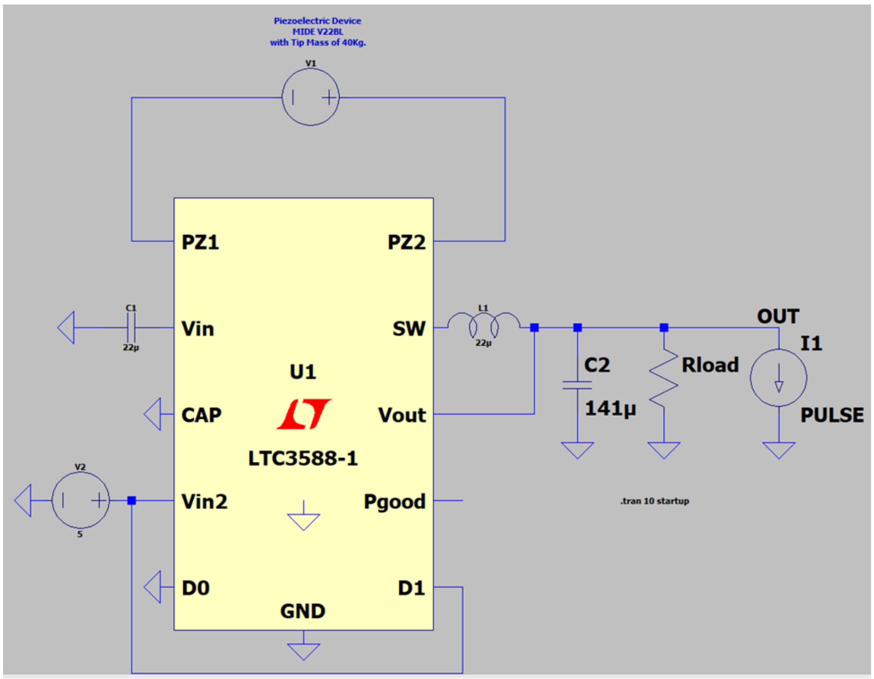

Figure 35: energy harvesting circuit using piezoelectric element

Figure 35 depicts the energy harvesting circuit using piezoelectric element for simulation using LTspice software. The circuit is designed in a way to put the piezoelectric effect in to the circuit.

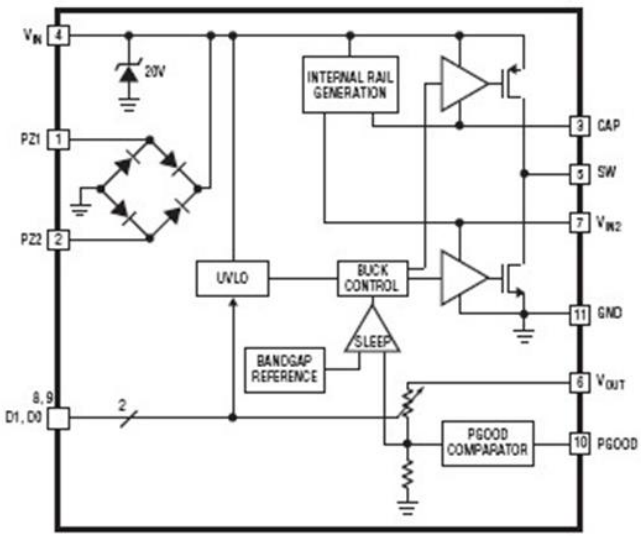

Figure 36: The circuit diagram of LTC388-1

The IC LTC388-1 as shown in Figure 36 is a piezoelectric energy harvesting power supply that is made of and ultra-low drop full wave rectifier which has a forward voltage drop of 400mV and it can withstand up to 50mA. The output of the full wave bridge rectifier will go into an input storage device. The circuit part showing a zener diode acts as a voltage clamp which clamps to voltage 20V on the input storage element and extracts excess energy above that to protect the device. Furthermore, the shunt current of the clamp circuit can carry 25mA from the input full wave bridge rectifier. Moreover, the D1 and D0 are two digital bits that are used to set the output voltage to 1.8V, 2.5V, 3.3V or 3.6V. There is a low current under voltage detector (UVLD) which controls the buck regulator. In addition, there are two input bias circuits to control the P-FET at the top and the N-FET at the bottom.

The circuit operates in such a way that as the input voltage in the input side storage element rises and goes beyond the under-voltage lockout rising threshold which 1.2V above the output setting, it turns on the buck regulator. It then turns on P-FET and it ramps the current to 250mA through the output inductor. At that instant, the P-FET turns off and N-FET turns on which ramps the current down to zero. By doing this, the charge from the input source is transferred to the output storage element. When the voltage across the input storage device gets down to 200mV above the output voltage setting, the buck regulator then turns off and goes into less than 10nA output current load and then it anticipated for the voltage to charge back up. After it charges back up above the under-voltage lockout rising, it turns the buck regulator back on. As the output voltage approaches the regulation point, the buck regulator will drive the output slightly above the regulation point at which it will enter sleep mode. During the sleep mode period, it presents less than 90nA of the output load to the output. The output then starts to decay due to leakage current. When the output drops slightly below the regulation point, the buck regulator turns back on and again charges up the output storage element.

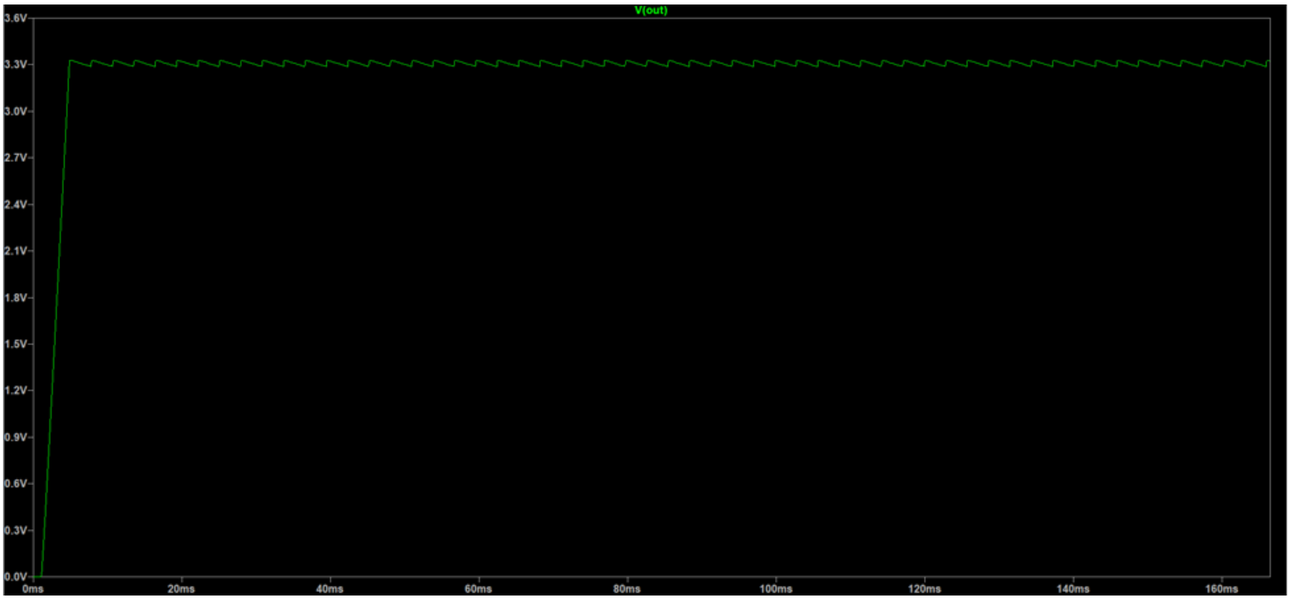

Figure 37: Output Voltage across the load

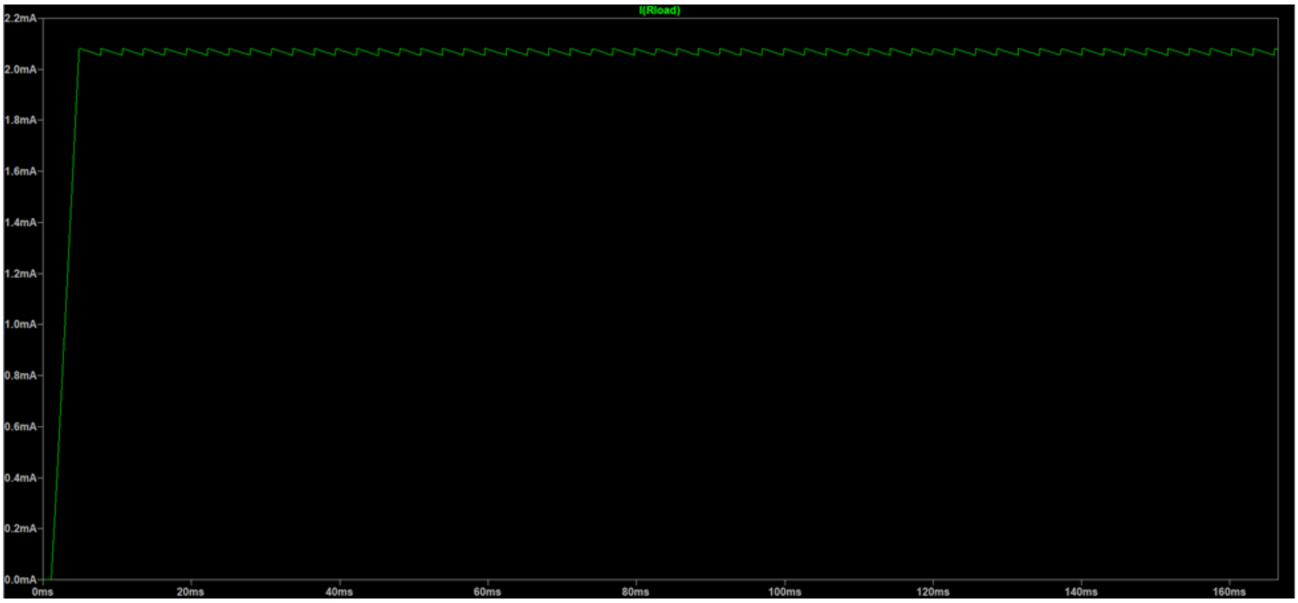

Figure 38: Output current through load

400 N mass was considered to be exerted and the corresponding voltage and current output were depicted in the graphs in Figure 37 and Figure 38 respectively.

Chapter 6

Feasibility Analysis

6.1 Impact and Sustainability

The project was designed in such a way that it can be run in any remote location where there is a lack of grid electricity supply. The system can also be modified to use in vehicles so that water can be available on the go resulting in an impact in the increase in production of clean water. Using this alternative method of water generation using renewable energy in mass scale can be a way to save underground water since it is decreasing very rapidly [3] . Again, the harmful pollution of burning natural resources for production of electricity can also be minimized to 70-90% compared with conventional power plants [39]. So, environmental sustainability is also ensured in this project.

6.2 Applicable Standard and Codes

Throughout the development phase of our project, we ensured that all the connection diagrams are first simulated and then hardware connection is given accordingly to prevent any short circuit or error in circuit. All the readings and parameters were taken very carefully to prevent any unwanted errors. We used QC passed quality solar panel to get appropriate data similar to simulation [40]. The AWG setup is also improved by trial and error in experimental setup. In measuring the current and voltage parameters of piezo and solar, a good quality multi-meter has been used and the least possible wire has been used to minimize the resistance. Overall, the whole work was done safely causing no harm to environment.

6.3 Risk Management and Safety Consideration

The design and planning of the project is done in such a way, it ensures the maximum protection of work and surrounding environment. While using the electrical appliances, we tend to use multimeters to measure voltage at every instant to ensure the safety of operations. Overheating, misconnections is cross checked before powering up and putting the system into operation. We have used insulated wires and proper connector in joints to prevent any unwanted shock and loss of energy [41]. Emission of harmful fumes will not occur in the process. Moreover, while using soldering iron, safety glasses and gloves has been used with appropriate soldering setup to prevent any unwanted accident as well as to increase the accuracy of soldering. Any wastage of materials and maintaining a clean workspace will be maintained.

Again, for the produced water, we will measure the safety concerns and take steps for identifying the issues to make it drinkable. The most efficient ways to produce maximum output in the least time is tested with care while modifying the equipment with added fan, fins and trying to make the system enclosed. Appropriate current and voltage display will show the status of operation in all instances and will give a sign if something unusual happens. Good quality cables and cable connectors has been used to prevent any overhear burnings and loose connections. All activities in design ensure that no overheating, short circuit take place and no fault exists in the system such that the system can be easily run.

Chapter 7

Conclusion and Future Work

7.1 Summary

Many obstacles were faced in the path of the project. Firstly, the pandemic limited the speed of work and perfect team collaboration. Experiments were done both though hardware and simulation work dived throughout the team. Our available resources found in this subcontinent are not much efficient with the actual product. We found this, from the efficiency rate of our Peltier device. Besides, the Piezo available also were not up to the mark and to get a suitable value we have to several tests and find the best possible use in the project. According to our geographical area, the results obtained for water accumulation are pretty much satisfactory. In other area of high humidity, the result will be much more significant.

7.2 Future Work

In future, we have a plan to set up a model of pure water stands at points of streets which will totally be run by solar power. The water extracted through this method is not drinkable due to the fact that the water is high in impurities and may cause adverse effects if consumed. Therefore, it is vital to provide a sample to the Department of Mathematics and Natural Sciences (MNS) as a future initiative to test the water for impurities at their microtechnology laboratory. This would provide necessary details on the impure substances in the water that require to be filtered in order to be drinkable. Another inclusion to the future work includes adding multiple Peltier and increasing the surface area for better results. Our present system can be developed better with 3D design structure giving rise to the water amount acquired from atmosphere. A major development in the future model is incorporating an automated switching phenomena between solar power generation system and battery depending upon solar irradiance. Overall future improvements aim for Improving the Energy- Water ratio.

References

[1] "Drinking-water," World Health Organization: WHO, 14 June 2019. [Online]. Available: https://www.who.int/news-room/fact-sheets/detail/drinking-water. [Accessed 20 October 2020].

[2] "What You Need to Know About the World's Water Wars," National Geographic News, 14 July 2016. [Online]. Available: https://www.nationalgeographic.com/news/2016/07/world-aquifers-water-wars. [Accessed 30 August 2020].

[3] A. Das, "Dhaka caving in alarmingly as groundwater level falls," 24 August 2016. [Online]. Available: https://www.theindependentbd.com/post/57286#:~:text=With%20the%20groundwater%20level%20continuing,dwindling%20supply%20of%20drinking%20water.. [Accessed 20 October 2020].

[4] "The End Of Fossil Fuel," Forbes, 24 July 2009. [Online]. Available: https://www.forbes.com/2009/07/24/peak-oil-production-business-energy-nelder.html?sh=5eee9ac24904. [Accessed 22 February 2021].

[5] H. A. Sodano, D. J. Inman and G. Park, "A Review of Power Harvesting from Vibration using Piezoelectric Materials," *The Shock and Vibration Digest*, vol. 36, no. 3, p. 197–205, 2004.

[6] Y. Alwokayan, H. Alabdulwahed, B. Alsader and Y. Alqallaf, "Solar Piezoelectric System," in *IEEE*.

[7] Z. Yang, S. Zhou and J. Zu, "High-Performance Piezoelectric Energy Harvesters," *Joule 2,* pp. 649-669, 2018.

[8] M. Singh, B. Yadav and A. Ranjon, "Synthesis and characterization of perovskite barium titanate thin film and its application as LPG sensor," *Sens. Actuators B 241,* p. 1170–1178, 2017.

[9] T. Anbarasu and P. Sekar, "Vapour compression Refrigeration system generating fresh water from humidity in the air," in *IET Conference Publications*, 2011.

[10] S. V.P, A. E.A, A. P, A. Vas C, B. Ibnu Masood, F. Ahamad and V. V.N, "PORTABLE ATMOSPHERIC WATER GENERATOR," *International Research Journal of Engineering and Technology (IRJET),* vol. 07, no. 04, pp. 1649-1652, 2020.

[11] S. C. B. R. K. E. Niewenhuis B., "Water generator water from air using liquid desiccant method," 2012.

[12] R. Atta, " Solar water condensation using thermoelectric coolers," *International Journal of Water Resources and Arid Environments,* vol. 1, no. 2, p. 142, 2011.

[13] A. Kabeela, M. Abdulazizb and M. Emad, "Solar-based atmospheric water generator utilisation of a freshwater recovery: A numerical study," 2014.

[14] A. Weidenkaff, "Thermoelectricity for future sustainable energy technologies," *EPJ Web of Conferences,* vol. 148, p. 10, January 2017.

[15] "Piezo Elements," All Electronics, 2018. [Online]. Available: https://www.allelectronics.com/category/466/piezo-elements/1.html. [Accessed 13 July 2021].

[16] S. J. Fonash, S. Ashok and R. T. Fonash, "Solar cell," Encyclopedia Britannica, 3 June 2020. [Online]. Available: https://www.britannica.com/technology/solar-cell. [Accessed 13 July 2021].

[17] "Arduino-Introduction," Arduino.cc, 2021. [Online]. Available: https://www.arduino.cc/en/guide/introduction. [Accessed 13 July 2021].

[18] "Arduino Uno Rev3 | Arduino Official Store," Arduino.cc, 2021. [Online]. Available: https://store.arduino.cc/usa/arduino-uno-rev3. [Accessed 13 July 2021].

[19] "DHT11 Sensor and Its Working," Elprocus, [Online]. Available: https://www.elprocus.com/a-brief-on-dht11-sensor/. [Accessed 13 July 2021].

[20] "Simulink Documentation," [Online]. Available: https://www.mathworks.com/help/simulink/. [Accessed 13 July 2021].

[21] "COMSOL - Software for Multiphysics Simulation," COMSOL INC., [Online]. Available: https://www.comsol.com/. [Accessed 13 July 2021].

[22] "Circuit Simulation softaware with SPICE," Proteus, [Online]. Available: https://www.labcenter.com/simulation/. [Accessed 13 July 2021].

[23] "Mixed Signal and Digital Signal Processing ICs," Analog Devices, [Online]. Available: https://www.analog.com/en/index.html. [Accessed 27 September 2021].

[24] A. Nechibvute, A. Chawanda and P. Luhanga, "Piezoelectric Energy Harvesting Devices: An Alternative Energy Source for Wireless Sensors," *Smart Materials Research*, vol. 2012, p. 13, 2012.

[25] S. Sherrit and B. Mukherjee, "Characterization of Piezoelectric Materials for Transducers," *Dielectric and Ferroelectric Reviews*, p. 45, 2007.

[26] E. Lefeuvre, D. Audiger, C. Richard and D. Guyomar, "Buck-Boost Converter for Sensorless Power Optimization of Piezoelectric Energy Harvester," *IEEE Transactions on Power Electronics,* vol. 22, no. 5, 2007.

[27] "Solar Charge Controllers," Morningstar Corporation, 2020. [Online]. Available: https://www.morningstarcorp.com/solar-charge-controllers. [Accessed 21 August 2021].

[28] M. Hussain, "Final Report of Solar and Wind Energy Resource Assessment (SWERA)-Bangladesh Project," SWERA – Bangladesh group, Dhaka, 2007.

[29] "Deep Cycle Battery FAQ," Northern Arizona Wind & Sun, [Online]. Available: https://www.solar-electric.com/learning-center/deep-cycle-battery-faq.html/. [Accessed 27 Septemeber 2021].

[30] "Solar Power Kits and Equipments for Sale," Renogy, [Online]. Available: https://www.renogy.com/. [Accessed 27 September 2021].

[31] T. Tritt, "Thermoelectric Materials: Principles, Structure, Properties, and Applications," *Encyclopedia of Materials: Science and Technology,* vol. 2, pp. 1-11, 2002.

[32] H. Jouharaa, A. Zabnienska-Gora, N. Khordehgah, Q. Doraghi, L. Ahmad, L. Norman, B. Axcell, L. Wrobel and S. Dai, "Thermoelectric generator (TEG) technologies and applications," *International Journal of Thermofluids,* vol. 9, February 2021.

[33] R. Akram Amarin, "HURRICANE WIND SPEED AND RAIN RATE RETRIEVAL ALGORITHM FOR THE STEPPED FREQUENCY MICROWAVE RADIOMETER," B.S. Princess Sumaya University for Technology, Florida, 2004.

[34] D. Bolton, "The Computation of Equivalent Potential Temperature," *Monthly Weather Review,* vol. 7, no. 108, pp. 1046-1053, 1980.

[35] D. Li and S. Kaewunruen, "Effect of Extreme Climate on Topology of Railway Prestressed Concrete Sleepers," *Climate-MDPI,* vol. 6, no. 17, 2018.

[36] "Relative Humidity Calculator," Lenntech, [Online]. Available: https://www.lenntech.com/calculators/humidity/relative-humidity.htm. [Accessed 27 September 2021].

[37] T. Kadhim, A. K. Abbas and H. J. Kadhim, "Experimental study of atmospheric water collection powered by solar energy using the Peltier effect," in *3rd International Conference on Engineering Sciences*, Kerbala, Iraq, 2020.

[38] "Bangladesh weather. Climate and weather in Bangladesh 2021," Hikersbay, [Online]. Available: http://hikersbay.com/climate/bangladesh?lang=en. [Accessed 27 September 2021].

[39] S. G, " Environmental Impacts of Renewable Energy Sources.," ADEC INNOVATIONS, 2017. [Online]. Available: http://blog.adecesg.com/blog/environmental-impacts-of-renewable-energy-sources. [Accessed 27 September 2021].

[40] B. Argetsinger and B. Inskeep, "Standards and Requirements for Solar Equipment, Installation,and Licensing and Certification-A Guide for States and Municipalities," Clean Energy States Alliance (CESA), 2017.

[41] O. Aneziris, I. Papazoglou, M. Konstandinidou, M. Damen, J. Kuiper, L. Bellamy, M. Mud, H. Baksteen and J. Oh, "Occupational Risk Management for Electrical Hazard," vol. 7, 2009.

Appendix

A. Water accumulation rate plotting on MATLAB

```
clear all;

close all;

clc;

time = [0, 1, 2 ,3 ,4 ,5 ,6];

Water_Amount = [0, 1, 2, 2.5, 3.5,5, 5.5];

time1 = [0, 1, 2, 3, 4, 5, 6];

Water_Amount1 = [0, 2.5, 4, 7, 8, 9, 9.5];

time2 = [0, 1, 2, 3, 4, 5, 6];

Water_Amount2 = [0, 4, 5, 6.5, 8, 10, 11.5];

time3 = [0, 1, 2, 3, 4, 5, 6];

Water_Amount3 = [0, 4.8, 10, 13.8, 16.2, 19.5, 25.5];

time4 = [0, 1, 2, 3, 4, 5, 6];

Water_Amount4 = [0, 25, 38, 57, 61, 82, 99];



hold on;

plot(time,Water_Amount,'r','LineWidth',2);

plot(time1,Water_Amount1,'b','LineWidth',2);

plot(time2,Water_Amount2,'y','Linewidth',2);
```

```
plot(time3,Water_Amount3,'g','LineWidth',2);

plot(time4,Water_Amount4,'black','LineWidth',2);

plot(time,Water_Amount,'*r', 'MarkerSize',5,'LineWidth',3);

plot(time1,Water_Amount1,'*b', 'MarkerSize',5,'LineWidth',3);

plot(time2,Water_Amount2,'*y', 'MarkerSize',5,'LineWidth',3);

plot(time3,Water_Amount3,'*g', 'MarkerSize',5,'LineWidth',3);

plot(time4,Water_Amount4,'*black', 'MarkerSize',5,'LineWidth',3);




xlabel('time(hour)');

ylabel('Water Amount(mL)');

title('Time vs. Water Amount');

grid on;
```

B. Code for Temperature and Humidity Sensing with DHT11

```
#include <dht.h>
#define dht_apin A0 // Analog Pin sensor is connected to DHT11 sensor;

void setup(){

  Serial.begin(9600);
  delay(500);//Delay to let system start
```

```
  Serial.println("DHT11 Humidity & temperature Sensor\n\n");
  delay(1000);//Wait before accessing Sensor

}//end "setup()"

void loop(){
  //Start of Program

    DHT.read11(dht_apin);

    Serial.print("Current humidity = ");
    Serial.print(DHT.humidity);
    Serial.print("%  ");
    Serial.print("temperature = ");
    Serial.print(DHT.temperature);
    Serial.println("C  ");

    delay(5000);//Wait 5 seconds before accessing sensor again.

  //Fastest should be once every two seconds.

}// end loop
```

C. MPPT algorithm for the specification Charge Controller

```
function duty = MPPT_algorithm(vpv,ipv,delta)

% I used the MPPT algorithm in the MATLAB examples

% I only modify somethings.
```

```
duty_init = 0.1;

% min and max value are used to limit duty between

% 0 and 0.85

duty_min=0;

duty_max=0.85;


persistent Vold Pold duty_old;

% persistent variable type can be store the data

% we need the old data by obtain difference

% between old and new value

if isempty(Vold)

    Vold=0;

    Pold=0;

    duty_old=duty_init;

end

P= vpv*ipv; % power

dV= vpv - Vold; % difference between old and new voltage

dP= P - Pold;% difference between old and new power


% the algorithm in below search the dP/dV=0

% if the derivative equal to zero
```

```
% duty will not change
% if old and new power not equal
% &
% pv voltage bigger than 30V
% the algorithm will works
if dP ~= 0 && vpv>30
    if dP < 0
        if dV < 0
            duty = duty_old - delta;
        else
            duty = duty_old + delta;
        end
    else
        if dV < 0
            duty = duty_old + delta;
        else
            duty = duty_old - delta;
        end
    end
else
    duty = duty_old;
```

```
end

%the below if limits the duty between min and max
if duty >= duty_max
    duty=duty_max;
elseif duty<duty_min
    duty=duty_min;
end

% stored data
duty_old=duty;
Vold=vpv;
Pold=P;
```

D. Code for relay switching

```
#include <LiquidCrystal.h>
const int rs = 12, en = 11, d4 = 5, d5 = 4, d6 = 3, d7 = 2;
LiquidCrystal lcd(rs, en, d4, d5, d6, d7);
// the setup routine runs once when you press reset:
void setup() {
  // initialize serial communication at 9600 bits per second:
```

```
  Serial.begin(9600);

  pinMode(13, OUTPUT);

  pinMode(8, OUTPUT);

  // set up the LCD's number of columns and rows:

  lcd.begin(16, 2);

  // Print a message to the LCD.

  lcd.print("The two voltages");

}


// the loop routine runs over and over again forever:

void loop() {

  // read the input on analog pin 0:

  int sensorValue = analogRead(A0);

  int sensorValue1 = analogRead(A1);

  // Convert the analog reading (which goes from 0 - 1023) to a voltage (0 - 5V):

  float voltage = sensorValue * (5.0 / 1023.0)* (12/5);

  float voltage1 = sensorValue1 * (5.0 / 1023.0)* (12/5);

  // print out the value you read:

  Serial.println(voltage);

  Serial.println(voltage1);

  lcd.setCursor(0, 1);
```

```
lcd.print(voltage);
lcd.setCursor(6, 1);
lcd.print(voltage1);
if(voltage>voltage1)
{

  digitalWrite(8, LOW);
  digitalWrite(13, HIGH);
}
else {
   digitalWrite(13, LOW);
   digitalWrite(8, HIGH);
}
}
```

E. Similarity Index Report

Present Report Details:

Submission date: 28-Sep-2021 07:47PM (UTC+0600)

Submission ID: 1659737675

File name: 7_18121018.pdf (2.14M)

Word count: 11757

Character count: 59108

7_18121018

ORIGINALITY REPORT

3%	1%	1%	2%
SIMILARITY INDEX	INTERNET SOURCES	PUBLICATIONS	STUDENT PAPERS

PRIMARY SOURCES

1	Submitted to Heriot-Watt University Student Paper	<1%
2	Submitted to University of Bahrain Student Paper	<1%
3	Submitted to University of Central England in Birmingham Student Paper	<1%
4	www.irjet.net Internet Source	<1%
5	Submitted to Napier University Student Paper	<1%
6	Submitted to Lebanese International University Student Paper	<1%
7	Submitted to Anglican Church Grammar School Student Paper	<1%
8	Submitted to Clayfield College Student Paper	<1%

9	Thualfaqir J. Kadhim, Abdalrazzaq K. Abbas, Hayder Jawad Kadhim. "Experimental study of atmospheric water collection powered by solar energy using the Peltier effect", IOP Conference Series: Materials Science and Engineering, 2020 Publication	<1 %
10	Sarker, Mahidur R., Azah Mohamed, and Ramizi Mohamed. "Modelling and Simulation an AC-DC Rectifier Circuit Based on Piezoelectric Vibration Sensor for Energy Harvesting System", Applied Mechanics and Materials, 2015. Publication	<1 %
11	instsignpost.blogspot.com Internet Source	<1 %
12	Submitted to Roehampton University Student Paper	<1 %
13	etheses.whiterose.ac.uk Internet Source	<1 %
14	Fabricio Hoff Dupont, Cassiano Rech, Jose Renes Pinheiro. "A methodology to obtain the equations for the calculation of the weighted average efficiency applied to photovoltaic systems", 2012 10th IEEE/IAS International Conference on Industry Applications, 2012 Publication	<1 %

Figure: Similarity Report of Present Report